Aus der Medizinischen Universitätsklinik und Poliklinik
Tübingen
Abteilung VII, Tropenmedizin
Schwerpunkt: Institut für Tropenmedizin, Reisemedizin,
Humanparasitologie

Analysing treatment failures by high-resolution capillary electrophoresis genotyping in uncomplicated *P. falciparum* malaria adapted from patient samples from Bobo-Dioulasso, Burkina Faso.

Inaugural-Dissertation
zur Erlangung des Doktorgrades
der Medizin

der Medizinischen Fakultät
der Eberhard Karls Universität
zu Tübingen

vorgelegt von

Nicklous, Raffaella Amber

2018

Dekan:	Professor Dr. I. B. Autenrieth
1. Berichterstatter:	Professor Dr. S. Borrmann
2. Berichterstatter:	Professor Dr. R. Klein
Tag der Disputation:	06.11.2018

Für meine Eltern.

LIST OF CONTENTS

LIST OF TABLES

LIST OF FIGURES

LIST OF ABBREVIATIONS & ACRONYMS

ACT	Artemisinin-based combination therapy
AL	Artemether-lumefantrine
ASAQ	Artesunate-amodiaquine
bp	Base pairs
CI	Confidence interval
DNA	Desoxyribonucleic acid
DP	Dihydroartemisinin-piperaquine
DSMB	Data Safety and Monitoring Board
ECG	Electrocardiogram
Fig.	Figure
GLURP	Glutamine-rich protein
H_E	Heterozygosity of infection
MOI	Mean multiplicity of infection
msp-1	Merozoite surface protein 1
msp-2	Merozoite surface protein 2
No.	Number
PA	Pyronaridin-artesunate
PCR	Polymerase chain reaction
P. falciparum	*Plasmodium falciparum*
pPCR	Primary polymerase chain reaction
rfu	Relative fluorescent units
sPCR	Secondary polymerase chain reaction
SD	Standard deviation

1 Introduction

"Malaria remains a major killer of children, taking the life of a child every two minutes." (World Health Organization 2016)

A considerable decline of incidence and mortality of malaria was achieved during the past years. Still, malaria remains one of the major health issues worldwide: in 2015, an estimated 212 million infections and 429 000 deaths, mostly of children aged 5 years or younger, were registered. The burden of malaria is disproportionately high in sub-Saharan Africa: 92 % of deaths from malaria are reported in this region. Burkina Faso belongs to the high transmission countries and is one of the poorest countries worldwide, which combines two major factors facilitating malaria (World Health Organization 2016).

Developing and evaluating new antimalarial drugs belongs to the most important instruments of fighting malaria. Genotyping of secondary infections after treatment is an essential tool to monitor the efficacy of antimalarial agents with high accuracy.

1.1 Malaria parasite

1.1.1 Discovery and classification

Malaria (deriving from the Italian *mal'aria* meaning "bad air") is caused by a protozoan parasite of the genus *Plasmodium*. Febrile diseases have been linked to swampy areas for thousands of years. However, the malaria parasite has been recognized as its cause only towards the end of the 19th century.

The first person to describe the parasite in human blood was Laveran in 1880. What followed in the next twenty years was research on the parasite's life cycle and its transmission: Ross was the first person to publish the full malaria life cycle in 1898 after having conducted several studies on avian Malaria and the Italian scientists Bignami and Grassi proved that the parasites are transmitted by inoculation of a female *Anopheles* mosquito (Cox 2010)(Ross 1898).

The life cycle of *Plasmodium* takes place both in the female *Anopheles* mosquito and in a human host. The *Anopheles* mosquito serves *Plasmodium* as a vector into the human body: by feeding on humans, it might inject one or several species of *Plasmodium* into the capillary system.

The human pathogenic species are

- *Plasmodium falciparum*
- *Plasmodium ovale*
- *Plasmodium vivax*
- *Plasmodium malariae*
- *Plasmodium knowlesi*

Malaria in humans can be caused by all of the listed *Plasmodium spp.* but the disease shows different characteristics depending on the infecting species. Whereas *Plasmodium ovale* and *Plasmodium vivax* are responsible for 48-hour fever attacks (*Malaria tertiana), Plasmodium malariae* evokes fever attacks every 72 hours (*Malaria quartana). Plasmodium vivax* and *Plasmodium ovale* are the only *Plasmodium spp.* to generate dormant liver stages, termed hypnozoites (Campo et al. 2015). These dormant liver stages induce relapses for up to a decade (Ashley & White 2014).

Plasmodium knowlesi has a shared reservoir between Southeast Asian macaques and humans. Up to 1971, only four authenticated cases of *Plasmodium knowlesi* malaria had been reported, but reports have been augmenting since 2004. Usually, *Plasmodium knowlesi* malaria results in uncomplicated malaria but it causes severe malaria in 10 % and is fatal in 1 – 2 % of cases (Millar & Cox-Singh 2015).

Malaria tropica on the other hand is characterized by irregular fever spikes and is caused by *Plasmodium falciparum (P. falciparum).* It can lead to severe malaria and it is responsible for 99 % of all malaria deaths (World Health Organization 2016). Below, I will focus on *P. falciparum* malaria due to its importance and high prevalence of 95 % of all malaria infections in Burkina Faso (Samadoulougou et al. 2014).

1.1.2 Life cycle of Plasmodium falciparum

Asexual stage in a human

The asexual stage of the protozoan's life cycle consists of a clinically silent pre-erythrocytic phase and a pathogenic intra-erythrocytic cycle: the pre-erythrocytic phase begins when the *Anopheles* mosquito inoculates a human with sporozoites. The sporozoites follow the bloodstream towards the liver and invade hepatocytes. They multiply as hepatic schizonts and produce several thousand merozoites, which are then released into the blood (Siciliano & Alano 2015). A single sporozoite can produce up to 30 000 merozoites (White et al. 2015). Merozoites invade red blood cells (RBC) by ligand-receptor-interactions and then develop from ring-stages to trophozoites to erythrocytic schizonts, which eventually release about 20 merozoites (Miller et al. 2002). These progenies re-enter the intra-erythrocytic cycle. The haploid set of 14 chromosomes is replicated by mitosis, whereas cell division (cytokinesis) occurs by a non-canonical process, termed schizogony. Few merozoites transform into sexual stages, the gametocytes.

Sexual stage in the female *Anopheles* mosquito

These female and male gametocytes can now be ingested by an *Anopheles* mosquito and consequently enable transmission. By feeding on an infected human being, the female *Anopheles* incorporates female and male gametocytes, which fuse and become a motile diploid zygote, the ookinete. This is the scene of meiotic replication and therefore exchange of genetic information between desoxyribonucleic acid (DNA) from the female and male gametocyte. The ookinete penetrates the *Anopheles'* gut wall and then transforms into an oocyst, in which thousands of sporozoites are produced. The oocyst bursts and releases the sporozoites, which migrate towards the anopheline salivatory glands (Siciliano & Alano 2015). With the next blood meal, the sporozoites are injected into the human host and a new asexual life cycle of *P. falciparum* begins.

Figure (Fig.) 1 depicts the life cycle of *P. falciparum.*

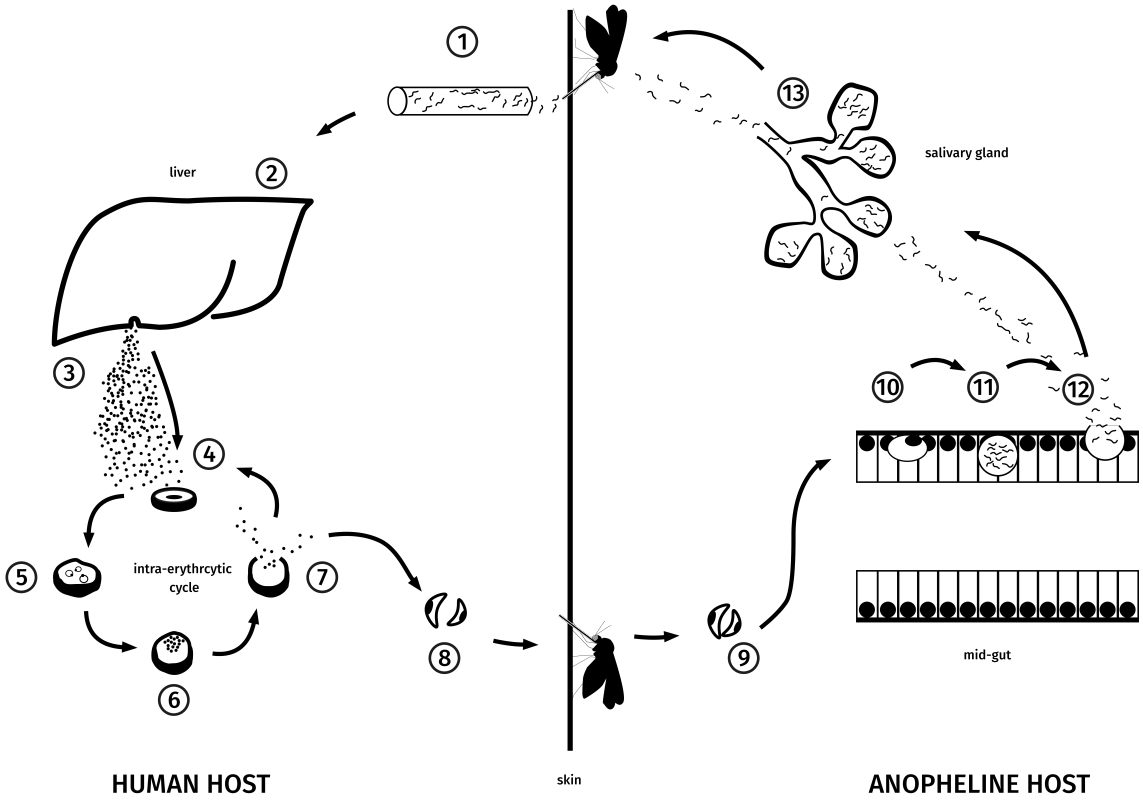

Figure 1: Life cycle of P. falciparum*. Asexual replication: (1) Sporozoites are inoculated by an Anopheles mosquito into a human host. The sporozoites travel in capillaries and vessels into the liver (2), where they penetrate hepatocytes and become liver-schizonts. The liver-schizonts burst and release merozoites (3), which penetrate red blood cells (4). In the red blood cells, the merozoites develop from ring stages (5) over trophozoites into blood-schizonts (6), which burst and release merozoites (7). Most merozoites enter a new red blood cell and repeat the intra-erythrocytic cycle. Few merozoites develop into female and male gametocytes (8), which are ingested by a female Anopheles during a blood meal. Transmission of P. falciparum is hereby enabled. Sexual stage: The microgametocyte and microgametocyte fuse into a zygote (9) and travel to the Anopheles' mid-gut. The zygote develops towards an ookinete (10) and further into an oocyst (11), which produces sporozoites. The oocyst bursts (12) and sporozoites travel towards the Anopheles' salivary gland, from where they are inoculated into a human host with the next blood meal.*

1.2 Prevention of malaria

1.2.1 Insecticide treated bed nets and indoor residual spraying

Insecticide treated bed nets (ITNs) and indoor residual spraying (IRS) with insecticides are fundamental methods of malaria control. Since *Anopheles* mosquitoes are mostly active during the night, sleeping underneath a bed net ensures protection against malaria in these hours. 53 % of the population at risk in sub-Saharan Africa slept underneath an ITN in 2015, and only 42 % of households held enough ITNs for each family member.

Resistance to pyrethroids, the insecticide used in ITNs, is increasing but studies show that ITNs remain effective (World Health Organization 2016).

1.2.2 Vaccines

P. falciparum undergoes various morphological and cell biological changes during its development in the human host, which leads to a strong variation of antigenic display (Arama & Troye-Blomberg 2014). The development of a highly protective vaccine has not yet been achieved, but several approaches have been developed; these can be sub-classified into transmission-blocking vaccines, pre-erythrocytic vaccines and blood-stage vaccines. A phase three trial of the pre-erythrocytic RTS,S/AS01 vaccine candidate showed insufficient protection of 55.8 % and 31.3 %, depending on age groups (The RTS,S Clinical Trials Partnership 2014)(The RTS,S Clinical Trials Partnership 2015). Newly published data from Tübingen show 100 % sterile protection in nine healthy, malaria-naive adults under chloroquine prophylaxis who were inoculated intravenously with chemoattenuated, non-irradiated *P. falciparum* sporozoite vaccine (Mordmüller et al. 2017). However, further clinical trials, including with heterologous challenge strains, have to be conducted.

1.3 Treatment of malaria

Antimalarial drugs have a long history. The first person to find an antimalarial chemotherapy was Paul Ehrlich in 1981, who found that methylene blue caused *Plasmodium* to vanish from the infected human's blood (Guttmann & Ehrlich 1891).
The alkaloid quinine was imported to Europe from South America in the 17th century as a component of the cinchona tree bark (Achan et al. 2011). It was isolated in 1820 and a century later, chloroquine and other synthetic antimalarial quinolones had been developed and were broadly distributed to treat malaria (Packard 2014). The spread of resistance to quinolines provoked further research on new antimalarial agents, which amongst others led to the isolation of artemisinin in the 1970s. Ever since the global introduction of artemisinin-based combination therapies (ACTs) starting around 15 years ago, these drugs have had a major impact on the containment of malaria and are the current first-line therapy of uncomplicated malaria.

1.3.1 Treatment of uncomplicated *P. falciparum* malaria

Uncomplicated *P. falciparum* malaria is defined by a positive blood smear and clinical malaria with no symptoms of severe malaria. Typical symptoms are high fever with ague, headache, fatigue and aching muscles. Uncomplicated malaria should be treated with an ACT (World Health Organization 2015).

Artemisinin-based combination therapies

Artemisia annua is a herb that has been used for centuries to cure fevers. The isolation of its antimalarial agent artemisinin in 1972 by Chinese scientists was an immense breakthrough in the fight against malaria (Klayman 1985) and was rewarded by the Nobel price for Youyou Tu in 2015. Artemisinin derivatives such as artemether, artesunate and dihydroartemisinin represent the antimalarials with the most potent anti-parasitic activity against all *Plasmodium* species (Makanga & Krudsood 2009)(White 2008). Once absorbed, all artemisinin derivatives convert into one active metabolite, dihydroartemisinin.

To reduce the risk of treatment failure with short (3-day) regimens, artemisinin derivatives are administered not as monotherapies but as artemisinin-based combination therapies (ACT). ACTs have been recommended by the World Health Organization since 2001 as first-line treatment against uncomplicated *P. falciparum* malaria. Combining partner drugs is based on several rationales: the combination of two antimalarial agents endows this combination with two different modes of action. Furthermore, artemisinin derivatives would have to be administered for seven days due to their short elimination half-life. Seven-day dosage schemes show little compliance and combining the artemisinin derivative with a different antimalarial with a longer elimination half-life facilitates a three-day treatment. The short-acting artemisinin derivative is associated with a high parasite reduction ratio and kills off a majority of the parasite's asexual stages effectively. As artemisinin derivatives have elimination half-lives of approximately one hour, they have to be combined with a more slowly eliminated partner drug, which shows a longer elimination half-life of more than one day to prevent recrudescent infections (Nosten & White 2007).

The modes of action of artemisinin derivatives are not yet fully understood, but there are several hypotheses on the mechanisms such as interference of the artemisinin

derivatives with plasmodial sarcoplasmic / endoplasmic calcium ATPase, interference with mitochondrial electron transport, interference with parasite transport proteins and unfolded protein responses. It is known that artemisinin derivatives kill most intra-erythrocytic parasite stages, including early ring stages, but have little effect on schizonts (ter Kuile et al. 1993).

The following ACTs were examined in the present thesis and are therefore described more into detail:

Artemether-lumefantrine

Artemether-lumefantrine (AL) belongs to the most frequently prescribed ACTs to treat uncomplicated malaria. Lumefantrine, an aryl amino-alcohol, shows an elimination half-life of 3.2 days (Ezzet et al. 2000). Drawbacks of AL are a twice-daily dosing scheme and the necessity of administering AL with fats to ensure good absorption of lipophilic lumefantrine.

Dihydroartemisinin-piperaquine

Piperaquine is a bis-quinoline and even though its mode of action is not fully understood, it is assumed to have similar effects on *Plasmodium* as chloroquine. The terminal elimination half-life for piperaquine is of 20 - 22 days (Sigma-Tau 2011), leading to a considerably long PTP (Pfeil et al. 2014). This advantage has to be weighed against the long exposure of re-infecting parasites to low piperaquine concentrations, which potentially leads to faster selection of less sensitive strains. Furthermore, higher gametocytaemia after treatment with dihydroartemisinin-piperaquine (DP) compared to AL has been observed, which increases the risk of transmission (Bassat et al. 2009).

Pyronaridine-artesunate

Pyronaridine has an elimination half-life of 14 – 18 days (Shin Poong 2017h), and therefore also provides a long PTP. (Sagara et al. 2016) published data, which indicates that PA is safe and well tolerated in re-treatment with pyronaridine-artesunate (PA). This data, as well as the data for the thesis at hand, originates from the WANECAM clinical trial, which was conducted in Westafrica from 2012 to 2015.

1.3.2 Treatment of severe malaria

Severe malaria is defined by presence of asexual *P. falciparum* parasitaemia and to name only the most important: coma, severe anemia and respiratory distress due to metabolic acidosis. If untreated, its case fatality rate is very high, and therefore should immediately be treated with intravenous or intramuscular artesunate for at least 24 hours. This medication is to be followed by a complete treatment with an ACT (World Health Organization 2015).

1.4 Monitoring antimalarial drug resistances

Resistance to antimalarial drugs is defined as the capability of a parasite to survive or replicate despite the administration and absorption of a drug given in a recommended dosage. A treatment failure on the other hand is defined as inability of an antimalarial agent to clear parasites or to cure clinical symptoms. Factors leading to 'apparent' treatment failure due to pharmacological factors include: non-compliance of the patient, incorrect dosage or poor quality of the antimalarial agent, drug interactions, low absorption for instance caused by diarrhea or vomiting, incomplete biotransformation of pro-drugs or rapid drug elimination in an individual (World Health Organization 2010).

Resistance to drugs arises due to two consecutive sequences. In terms of evolution a *de novo* mutation occurs bearing a selection advantage that protects the parasite from the antimalarial agent. Having acquired this survival advantage and therefore being less sensitive to the drug, this parasite can multiply. If resistant parasites differentiate into gametocytes, these parasites can then be transmitted by *Anopheles* mosquitoes and disseminated to a broader population, giving rise to global spread of resistant alleles (Wootton et al. 2002)(Roper et al. 2004)(World Health Organization 2010).

After the large spread of resistance to chloroquine and pyrithamine in the 20th century, artemisinin tolerance has spread in Southeast Asia in the past decade (Noedl et al. 2009)(Dondorp et al. 2010)(Ashley et al. 2014). A small, albeit significant decline in early response rates observed in a previous study in Kilifi District indicated that artemisinin tolerance may also emerge or spread in sub-Saharan Africa (Borrmann et al. 2011). Two points are important to note. First, artemisinin tolerance is characterized by the ability particularly of young ring stage parasites to survive spikes of high drug

concentrations *in vitro* (measured by the ring stage survival assay, RSA) – this results in slower than normal clearance of blood stage parasites from the circulation *in vivo* and thus a delayed clearance phenotype (Witkowski et al. 2013). Second, it appears that this phenotype is not due to a single point mutation but to several point mutations in the propeller domain of the kelch13 gene and that these mutations have arisen independently in different geographical locations (Ashley et al. 2014).

It is therefore of great importance to contain the spread of resistance against artemisinins in an early stage. Monitoring antimalarial drug efficacy and drug resistances are therefore essential tools and are implemented on different levels:

- *Ex vivo / in vitro* assessment of sensitivities of cultured *P. falciparum* parasites serve as an early warning system to resistances. Different drug concentrations are administered to cultured *P. falciparum* parasites to observe the behavior of the parasite to the drug.
- The research on molecular markers of genetic mutations of the parasite is an accurate detection method and allows population-level screening for resistances.
- The benefit from pharmacokinetic analyses is its power to discriminate between true drug resistance and improper or inadequate drug exposure. Furthermore, it can uncover the necessity of dose adjustment of the antimalarial agent.
- The execution of clinical trials measuring clinical and parasitological efficacy of medications is a crucial method to notice changes in treatment outcome and has become the gold standard for monitoring drug resistances. Genotyping treatment failures corrects the efficacy results by distinguishing real treatment failures (recrudescences) from new infections and is recommended by the World Health Organization as a crucial tool in drug trials.

1.4.1 Genotyping

Genotyping is a fundamental tool to distinguish recrudescences from new infections in antimalarial drug trials and to assess polymerase chain reaction (PCR) – corrected treatment failure rates (World Health Organization 2008). Furthermore, the number and types of simultaneously occurring genotypes can be investigated. The pretreatment blood sample of an individual is paired to the patient's blood sample from the day of

recurrence of clinical malaria. Highly polymorphic gene loci of *P. falciparum* are amplified, marked with fluorescent dye and detected by capillary electrophoresis (CE).

The formerly used gel electrophoresis is being replaced by CE genotyping using automated deoxyribonucleid acid (DNA) sequencers. CE has far better resolution compared to standard gel electrophoresis. The length of fragments can be determined with a precision of one to three base pairs (bp). In contrast, using gel electrophoresis, genotypes are aggregated into 20 – 40 bp bins and as a result misclassifications can occur. CE also shows an advantage in detecting multiple infections (Falk et al. 2006) and in analysing samples with high parasite densities (Liljander et al. 2009). However, the main drawback of CE genotyping is the high cost of automated sequencers. Thus, gel electrophoresis remains an important tool in field settings when CE genotyping is not available, especially as the efficiency of differing recrudescent genotypes from new infections is alike whether gel electrophoresis or CE is performed (Liljander et al. 2009).

Merozoite surface protein 2

Highly polymorphic gene loci encoding merozoite surface proteins such as merozoite surface protein 1 (msp-1), merozoite surface protein 2 (msp-2) or glutamine-rich protein (GLURP) show above-average genetic diversity due to diversifying immune selection pressure. This renders msp-1, msp-2 and GLURP suitable for genotyping of *P. falciparum* field isolates. As msp-2 shows the highest discriminatory power (Basco et al. 2004), it is an ideal genetic marker and was used in this study to investigate treatment failure rates.

The exact function of msp-2 has not yet been identified but studies indicate it to be important when merozoites bind to erythrocytes. Moreover, it has been suggested that surface proteins play a variety of roles while entering an erythrocyte and afterwards (Boyle et al. 2014).

Msp-2 is located on chromosome 2 (Wickham et al. 2003). The genetic locus coding for msp-2 can be sub-classified into five blocks as can be seen in Figure 2. Block one and five are highly conserved N- and C-terminal regions. Block two and four are non-repetitive variable regions and block three consists of a highly polymorphic central region (Smythe et al. 1991) (Kiwanuka 2009), which occurs as one of two dimorphic

allelic families: 3D7-type alleles and D10-type alleles (Smythe et al. 1991). In literature, 3D7 is often referred to as IC-1 and D10 as FC27 (Wickham et al. 2003). The sequence diversity within each allelic family concerns the repeat regions and the regions flaking these (MacRaild et al. 2015). The allelic families differ in nucleotide sequences on the one hand and in the quantity of repetitive sequences on the other hand (Joshi et al. 2007). Below, these individually sized fragments, which can be allocated either to 3D7 or D10, will be referred to as genotypes.

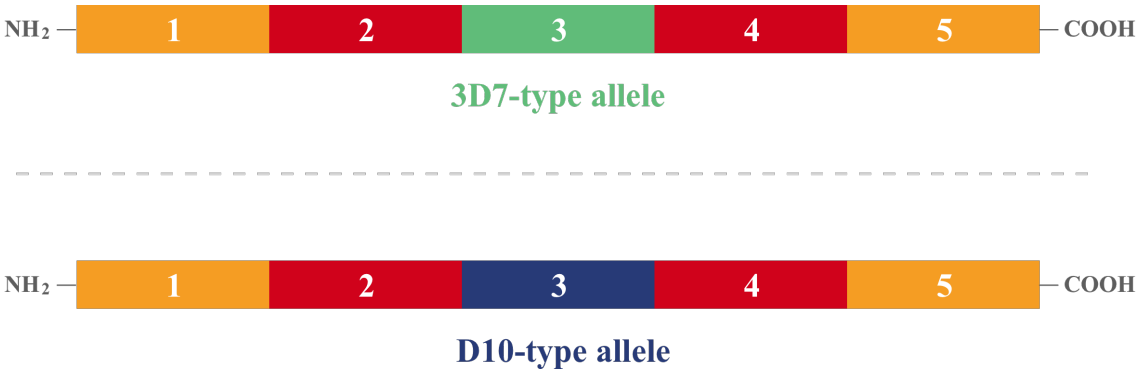

Figure 2: Scheme of the genetic composition of the merozoite surface protein 2 on chromosome 2. Block 1 and 5 (yellow) are highly conserved terminal regions, whereas block 2 and 4 (red) are non-repetitive variable regions. Block 3 is composed as highly polymorphic central region and occurs as 3D7-type allele (green) or as D10 type (blue) allele.

1.5 Aim of the study

In this pilot study, I examined 63 paired samples from the WANECAM-trial with the title "*A Phase IIIb / IV comparative, randomized, multi-centre, open label, parallel 3-arm clinical study to assess the safety and efficacy of repeated administration of pyronaridine-artesunate, dihydroartemisinin-piperaquine or artemether-lumefantrine or artesunate-amodiaquine over a two-year period in children and adult patients with acute uncomplicated Plasmodium sp. malaria.*" by high resolution capillary electrophoresis genotyping of *P. falciparum* msp-2.

For the first time, malaria samples from Bobo-Dioulasso, Burkina Faso were examined by high resolution CE genotyping. Genotyping has become an important method in antimalarial drug trials and it was therefore of major interest to establish this method for samples from the WANECAM-trial. My hypothesis was that it was possible to establish high resolution CE genotyping for these samples. My main study aim was to distinguish

recurrences in whether they appeared due to a new infection or due to recrudescence. Secondary outcomes concerned the assignment of recrudescences to treatment arms and to certain alleles. Moreover, allele frequencies were investigated.

2 Materials & Methods

2.1 Materials

2.1.1 Samples

Filter paper blood samples were taken from patients from Bobo-Dioulasso, who were enrolled in the WANECAM drug-trial. Each patient was followed-up for 42 days and on each visit finger prick blood samples were collected on Whatman™ 3MM filter papers. The filter papers were dried and stored separately in sealed plastic bags to prevent cross contamination. The bags, containing silica gel to prevent humidity, were stored at room temperature. 63 paired samples from patients, who had suffered a treatment failure within 42 days, were placed to my disposal by my Burkinian colleagues. 59 of the 63 paired samples derived from the study site in Sakaby, including 48 paired samples from the AL study arm, 6 paired samples from the DP study arm and 5 paired samples from the PA study arm. 4 paired samples, all from the AL study-arm, derived from the study site in Colsama. All samples were transported by plane to Tübingen, Germany, and analysed in the laboratory of Professor Borrmann.

2.1.2 Enzyme

Table 1: Enzyme used for PCR.

Thermo Scientific	*Taq* DNA Polymerase (recombinant) 5 U / µl, 500 U

2.1.3 Synthetic oligonucleotides

Table 2: Synthetic oligonucleotides.

Name	**Company**	**Sequence**	**Vol. for 100 pmol / µl**	**Molarity**
dNTP Mix	Thermo Scientific	dNTP Mix Molecular Biology Grade		2 mM each

Msp-2 S1	Eurofins Genomics	5'-gtctcttcttataatatgagtataaggagaa 3'(31)	178 µg	18.5 nmol
Msp-2 S2	Eurofins Genomics	5'-gaaggtaattaaaacattgtc 3' (21)	150 µg	23.1 nmol
Msp-2 S3	Eurofins Genomics	5'-gagggatgttgctgctccacag 3' (22)	165µg	24.3 nmol
M5	Eurofins Genomics	FAM 5'-gcattgccagaacttgaa 3' (18)	277µg	45.8 nmol
N5	Eurofins Genomics	JOE 5'-ctgaagaggtactggtaga 3' (19)	409µg	62.1 nmol

2.1.4 Size standards

Table 3: Size standards.

Size Standard Name	Company
100 bp DNA ladder N323L Size Standard	New England Biolabs
Gene Scan™ –500, ROX™ Size Standard	Applied Biosystems

2.1.5 Antimalarial agents

Table 4: Antimalarial agents.

Antimalarial Agent	Registered Trade Name	Company
Artemether-lumefantrine	Coartem®	Novartis Pharmaceutical Cooperation
Dihydroartemisinin-piperaquine	Eurartesim®	Sigma-Tau Pharma
Pyronaridine-artesunate	Pyramax®	Shin Poong Pharmaceutical

2.1.6 Chemicals

Table 5: Chemicals.

Chemical Name	Company
Boric acid for analysis	Emsure Acs Iso Reag. Ph Eur Merck KGaA Darmstadt

86 – 88 % Ethylendiaminetetraacetic acid (EDTA) $C_{10}H_{12}N_2Na_4O_8$	Carl Roth GmBH + Co KG Karlsruhe
3130 POP-7™ Performance Optimized Polymer	Applied Biosystems
Hi-Di™ Formamide	Applied Biosystems
SeaKem LE Agarose	LONZA
SybrGreen® I 2 x 500 µl	Biozym
Trishydroxylmethylaminomethane Tris Ultrapure $C_4H_{11}NO_3$	AppliChem Panreac ITW companies, Darmstadt

2.1.7 Buffers, media and solutions

Table 6: Buffers, media and solutions.

Content	**Company**
10X Sequencer Buffer with EDTA	Applied Biosystems
10X *Taq* – buffer with $(NH_4)_2SO_4$	Thermo Scientific
25 mM $MgCl_2$	Thermo Scientific
LiChrosolv® Water for Chromatography	Merck KGaA
Loading – buffer	Life technologies

2.1.8 Disposables

Table 7: Disposables.

Name	**Company**
Eppendorf Sterile Biopur 1.5 ml tubes	Eppendorf
Micro Tubes 0.5 ml, PP	Sarstedt
Parafilm “M” Laboratory Film	Pechiney Plastic Packaging
PCR SingleCap 8er-SoftStrips 0.2 ml	Biozym Scientific
Plate Septa 96-Well	Applied Biosystems
Quali-PCR-Plates G060/H-1E-OA	Kisker Biotech
SafeSeal Micro Tube 2 ml, PP	Sarstedt
TipOne 200 µL Graduated Filter Tip	Starlab

(Sterile)

2.1.9 Equipment

Table 8: Equipment.

Equipment Name	Company
3130 / 3130 *xl* Genetic Analyzers	Applied Biosystems
Bench DNA/RNA UV-Cleaner UVC/T-M-AR	Kisker Produkte für Biotechnologie
Centrifuge Galaxy Mini	VWR International
Centrifuge Megafuge 1.0R	Heraeus
Mastercycler epgradient S	Eppendorf
Eppendorf Research 1000 µl Pipettes	Eppendorf
Eppendorf Research 200 µl Pipettes	Eppendorf
Eppendorf Research 10 µl Pipettes	Eppendorf
Eppendorf Research 2.5 µl Pipettes	Eppendorf
Freezer - 18 °C: Premium NoFrost	Liebherr
Heater and Magnet Mixer MR 3001	Heidolph
HG Tuning-Fork Scale Max/d 2000/0.01g	Vibra Shinko Denshi
Lab dancer	IKA
MicroAmp™ Optical 96-Well Reaction Plate	Applied Biosystems
neoBlock – HeizerDuo 2-2504	neoLab
Plate Septa 96-Well	Applied Biosystems
PowerPac™ Basic 300V/400mA/75 W	Bio-Rad
Refrigerator: Premium	Liebherr
Run 3130 Data Collection v 3.0 Properties	Applied Biosystems
Subcell GT Cell Electrophoresis Systems	Bio-Rad
Vortex Mixer VM 300	neoLab 7-2020

2.1.10 Software

Table 9: Software.

Name	Company
BioDocAnalyze	Biometra
Excel	Microsoft
Gene Mapper® v 4.0 Properties	Applied Biosystems
GraphPad PRISM® 7	GraphPad Software, Inc.
Mendeley	Elsevier
Powerpoint	Microsoft
Word	Microsoft

2.2 Methods

2.2.1 Study design

The WANECAM drug trial with the title "*A Phase IIIb / IV comparative, randomized, multi-center, open label, parallel 3-arm clinical study to assess the safety and efficacy of repeated administration of pyronaridine-artesunate, dihydroartemisinin-piperaquine or artemether-lumefantrine or artesunate-amodiaquine over a two-year period in children and adult patients with acute uncomplicated Plasmodium sp. malaria.*" was undertaken in Burkina Faso, Guinea Conakry and Mali (Clinical trial registry: PACTR20115000286876). 744 patients were included in Bobo-Dioulasso, of which 296 were recruited for AL and 224 for DP and PA, respectively. DP and PA were compared to AL. The comparator artesunate-amodiaquine (ASAQ) was not used in Bobo-Dioulasso. The enrolment period in Bobo-Dioulasso took place from August 2012 until December 2015. Each patient was followed for two years and treated with the same study drug if a new malaria episode occurred.

2.2.2 Study endpoints

The primary objective of the WANECAM study was to compare the incidence rate of uncomplicated malaria in children and adults who were treated repeatedly over a period

of two years with the same ACT. A primary efficacy endpoint was to show the non-inferiority of PA and DP compared to AL or ASAQ.

One of several secondary endpoints was to assess the PCR-corrected treatment failure rate by genotyping. The study investigated whether recurrent infections occurring within a follow-up period of 42 days derived from new infections or from persistent primary infections (recrudescences).

2.2.3 Study site

Burkina Faso is a landlocked West African country, which borders clockwise on Niger, Benin, Togo, Ghana, Ivory Coast, and Mali. Its surface is 273,000 km² and in 2016, its population was estimated at 18,634,000 inhabitants. The GDP per capita in 2014 was of 725 US $ (UNdata 2016f). Burkina Faso's official language is French but many local languages such as Dioula, Mooré and Foufouldé are spoken.

Burkina Faso was politically stable for many years. This changed when the former president Blaise Compaoré, who is known to have assassinated his friend, revolutionist and national hero Thomas Sankara, was about to change a law that would have allowed him a fifth mandate after having been in power for 27 years. Strikes and demonstrations climaxed in the resignation of Compaoré on October 31st, 2014 (ZEIT ONLINE 2017b). An interim government was installed but it suffered a military coup on September 23rd, 2015 in which its transitional president Kafando was held captured amongst others. The coup was organized by the former presidential guard under the lead of Gilbert Diendéré but was calmed by the agreement, which determined that Compaoré's allies were allowed to run for the presidential office during the upcoming elections (ZEIT ONLINE 2017c)(LeMonde 2017e). Finally, on November 29th, 2015 Roch Marc Christian Kaboré from the People's Movement for Progress won the election with nearly 53.5 % and became the current president of Burkina Faso (FAZ 2017d).

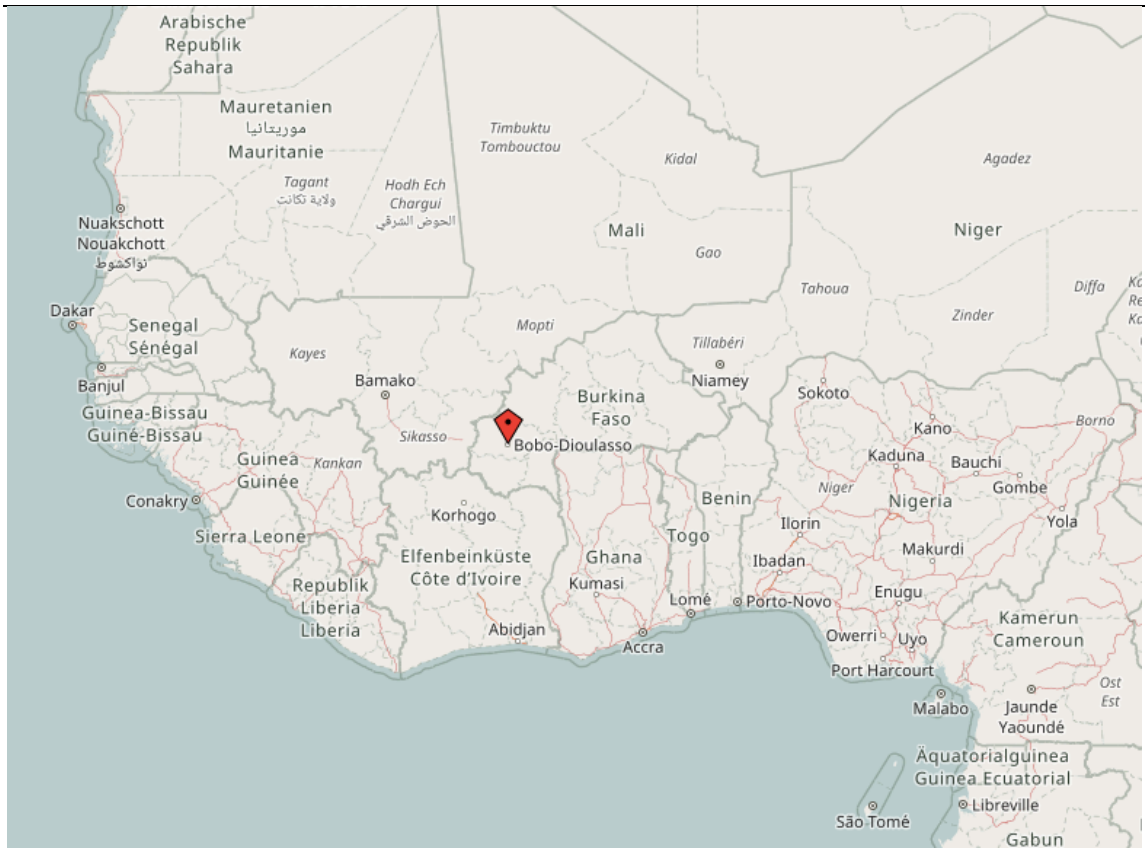

Figure 3: Map of Westafrica, highlighting the city Bobo-Dioulasso. © OpenStreetMap contributors

Bobo-Dioulasso is Burkina Faso's second largest city after the capital Ouagadougou and the economic heart of the country. It is situated in the region of Hauts-Bassins in the province of Houet about 350 km from Ouagadougou. It has a population of approximately 813 610 inhabitants in the census of 2012 (DGESS 2014)(ISND 2017g). The rainy season arises from June to November, which leads to a malaria transmission time of approximately eight months in Bobo-Dioulasso (Tinto et al. 2016). The annual entomological inoculation rate was estimated by 60 infective bites per person per year (Tinto et al. 2002), which characterizes mesoendemic transmission (Kiwanuka 2009).

A first study site was installed with the beginning of the study in 2012 in Sakaby, a small town in the northern surroundings of Bobo-Dioulasso. To accelerate the recruitment rate, a second study site was established in Colsama in the southwestern part of Bobo-Dioulasso. Both study sites were established in local dispensaries. To see were the study sites were located, see Figures 4 – 6.

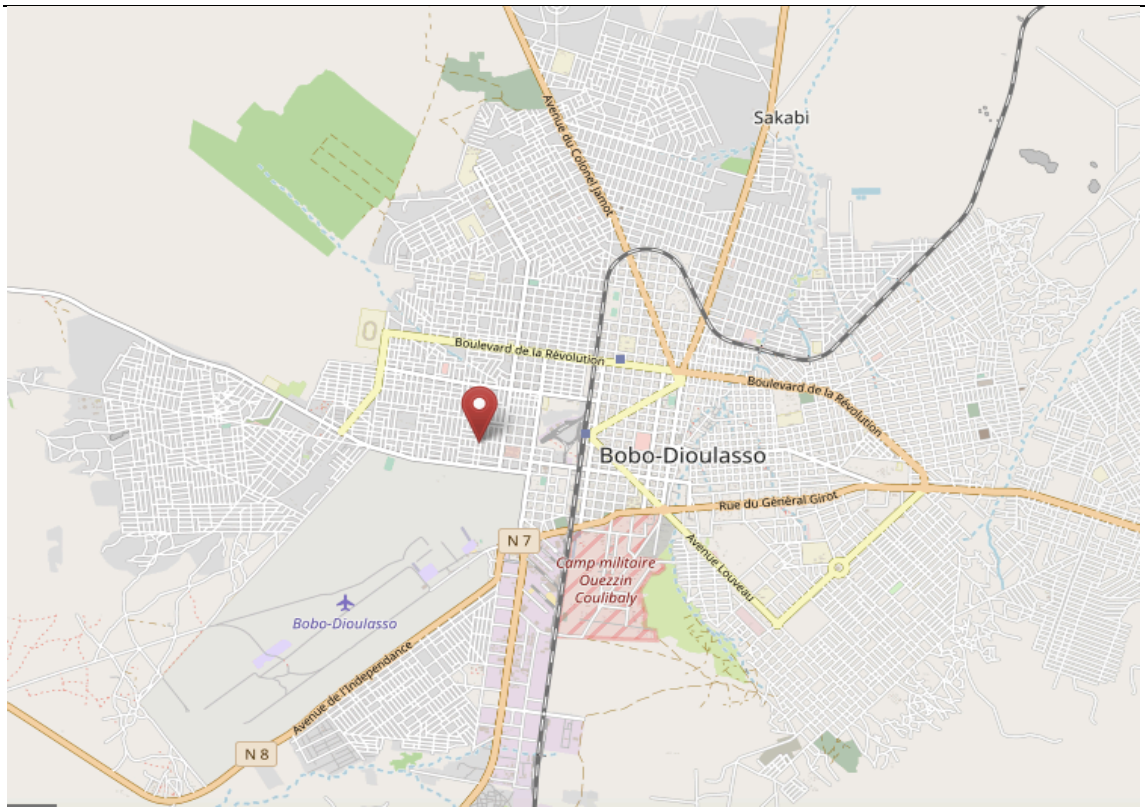

Figure 4: Streetmap of Bobo-Dioulasso indicating the local dispensary CSPS de Colsama in the west of Bobo-Dioulasso. © OpenStreetMap contributors.

Figure 5: Photography of the local dispensary and study site, CSPS Colsama, Bobo-Dioulasso.

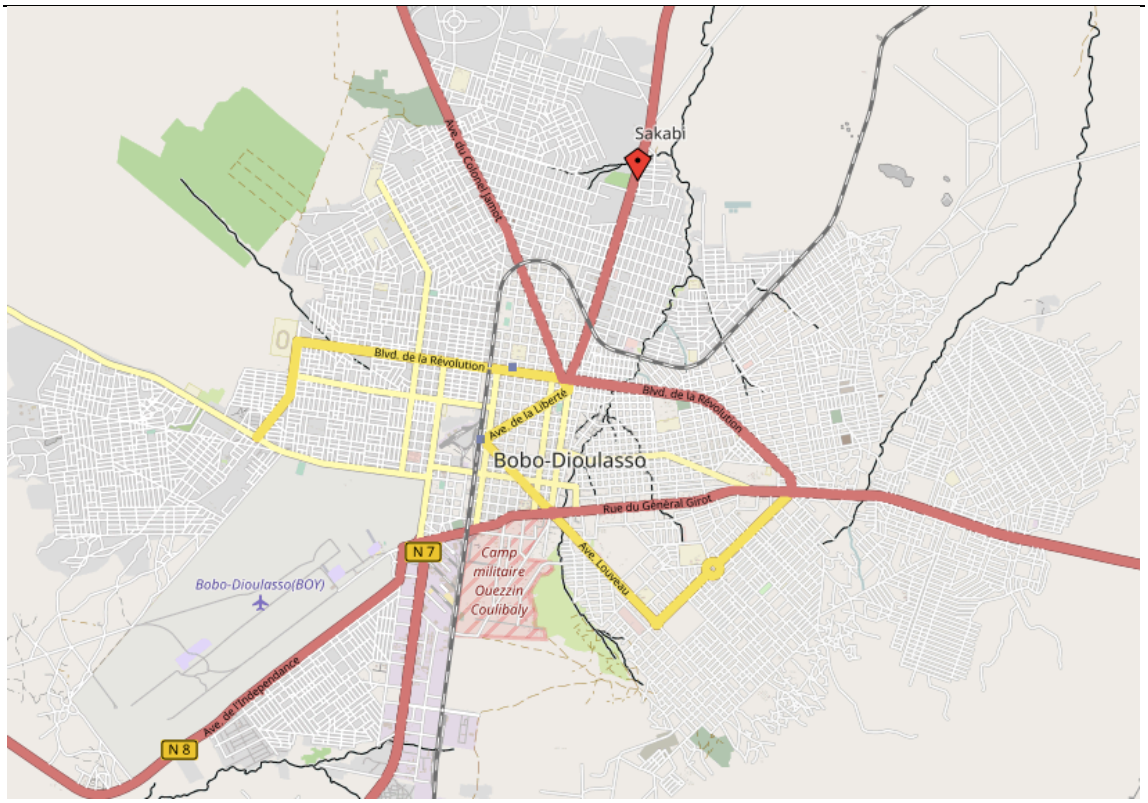

Figure 6: Streetmap of Bobo-Dioulasso indicating the local dispensary CSPS de Sakaby in the north of Bobo-Dioulasso. © OpenStreetMap contributors

2.2.4 Patients

Patients coming to the study sites lived within a radius of approximately zero to four kilometers. They arrived mostly by foot, but a few were driven by a fieldworker. Each patient was enrolled in the study for two years of follow-up.

The patients were blindly assigned to treatment arms. If patients fulfilled all inclusion-criteria, they were assigned to the lowest available number on the randomisation list. Every number on the randomisation list contained an attribution to one of the following study medications: AL, DP or PA. Each patient was treated for three consecutive days. On each day of treatment and during every follow-up visit a physician conducted a physical examination, a questionnaire was answered, blood smears were analysed and filter paper blood samples were taken. Biochemical and hematological parameters were investigated on day 0, 3 and 28. An electrocardiogram (ECG) was written on day 0 and day 2 with special attention to significant QT-prolongations or arrhythmias. Table 10 illustrates the visit schedule for enrolled patients.

Table 10: Visit schedule for enrolled patients.

Day	0	1	2	3	7	14	21	28	35	42
Treatment	☑	☑	☑							
Clinical examination	☑	☑	☑	☑	☑	☑	☑	☑	☑	☑
Malaria blood smears	☑	☑	☑	☑	☑	☑	☑	☑	☑	☑
Filter paper samples	☑	☑	☑	☑	☑	☑	☑	☑	☑	☑
Biochemistry	☑			☑				☑		
ECG	☑		☑							

The patients or parents in case of paediatric patients were asked to come to the clinic at any time if they felt ill. If a second clinical malaria infection occurred within the follow-up phase of 42 days, this was managed as a treatment failure. If a second clinical malaria infection occurred after the follow-up period of 42 days, the event was registered as a consecutive malaria episode. In case of a new uncomplicated malaria episode, patients were treated with the same medication as in their first episode.
More details on the WANECAM-trial can be seen in the appendix.

2.2.5 Pilot study – summary

I familiarized myself with the protocol for high-resolution capillary electrophoresis genotyping at the AG Borrmann laboratory, Institute for Tropical Medicine in Tübingen, to analyse 63 paired samples that were assigned to me by my Burkinian colleagues at the end of my stay. All samples derived from patients who were enrolled in the WANECAM-study in either Sakaby study site or Colsama study site.
I examined these 63 paired samples from Bobo-Dioulasso to differentiate recrudescences from new infections in treatment failures before day 42. A new infection is defined as a consecutively appearing parasitaemia with no common allele between day 0 and the day of recurrence. A recrudescence is defined as persistence of at least one allele from day 0 (World Health Organization 2008).
I extracted DNA from the filter paper blood samples and then I amplified the DNA in a nested polymerase chain reaction (Figure 7): First, I performed a primary PCR (pPCR) using primers that bind to the conserved flanking regions of block 3 of msp-2. Next, I

performed a secondary PCR (sPCR) with family-specific primers to amplify variable-size fragments using one fluorescence-marked primer per family-specific PCR reaction. I determined presence or absence of the PCR product by agarose gel electrophoresis to verify the success of my PCR reaction. In case of a positive result, I further analysed these samples in an automated sequencer (3130 / 3130 xl Genetic Analyzers, Applied Biosystems). I used the software GeneMapper® 4.0 for examining the results and inspecting the electropherograms. Genotying was performed in accordance with the genotyping protocol from Falk *et al.* (2006).

2.2.6 DNA extraction

The first step of my experimental laboratory work was to extract the DNA contained in dried filter paper blood samples, which I had collected from patients in Bobo-Dioulasso. The DNA extraction was performed underneath a laboratory hood used exclusively for genomic DNA (gDNA) extraction. The extraction was performed wearing gloves. To begin with the extraction, I cut two to three stripes of about 3 - 5 mm length and 1 mm width into a 0.5 µl tube. With each new sample I changed gloves and disinfected the scissors with 95 % alcohol. I introduced one DNA-free tube as a negative control, which was handled exactly as the other tubes. I added 100 - 150 µl of methanol to each tube to fix the DNA and left the tubes open overnight, which caused the methanol to evaporate. To lower the risk of contamination, the hood was closed during this step. The next morning I adjusted a heater to 100 °C and I added 100 – 150 µl of nuclease-free water to the tubes. I closed all lids of the tubes and boiled them for 15 minutes. Within this time I vortexed each tube at least three times for 20 – 30 seconds starting after 5 minutes of heating. Heating and vortexing the tubes caused the DNA to pass from the dried filter paper into the water so that I could select and amplify *Plasmodium* DNA in the following steps.

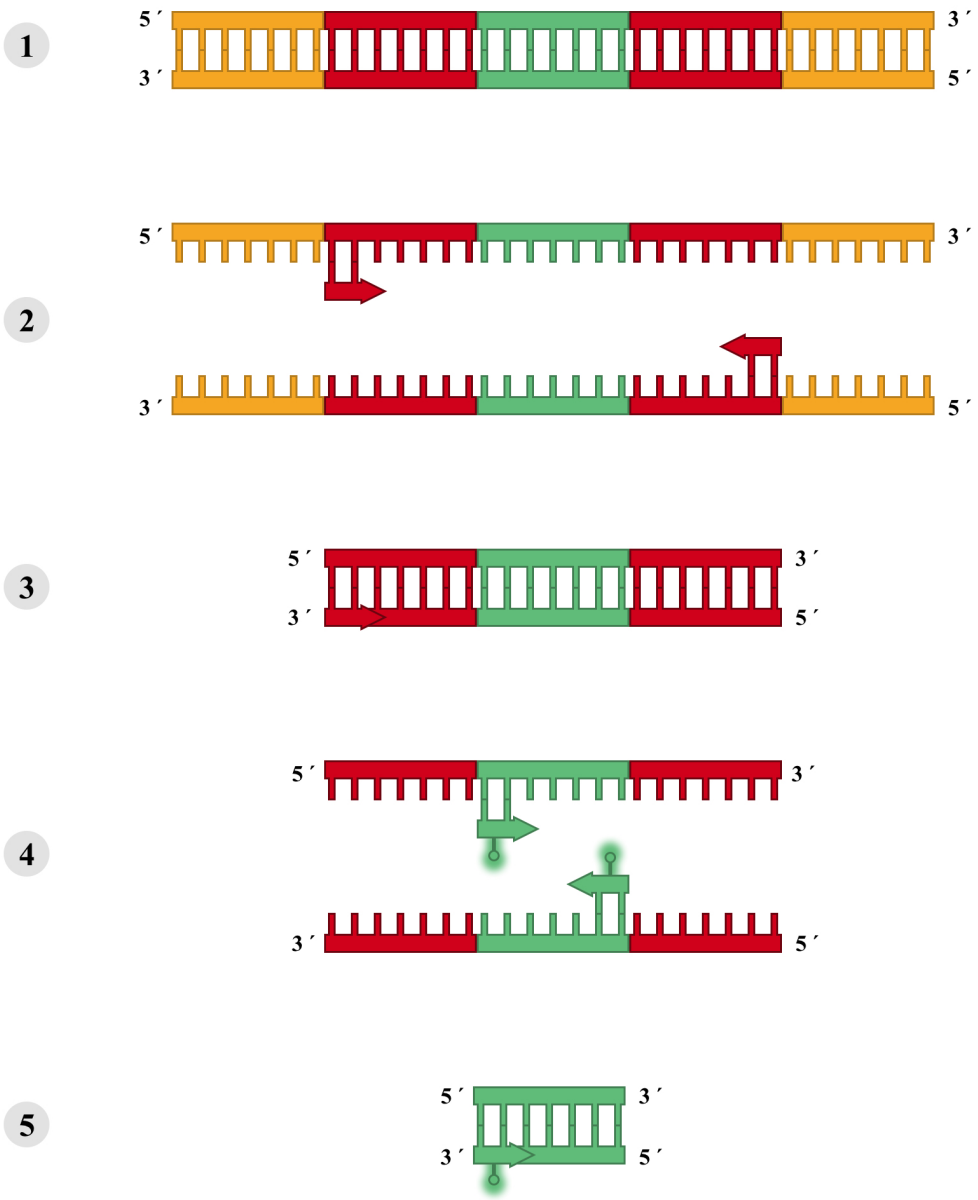

Figure 7: Nested PCR, consisting of pPCR (steps 1 – 3) and sPCR (steps 3 – 5). P. falciparum DNA is heated, thereby the hydrogen bonds dissolve and both DNA strands can be used as template for new amplification (step 1). Primers from pPCR (red) bind to the flanking regions of block three of msp-2 and Taq-polymerase begins the amplification using nucleotides. As the pPCR primers bind to the flanking region of block three of msp-2, the amplicon is shorter than the original template (step 3). In sPCR, the short amplicon from step 3 is heated again. Hydrogen bonds dissolve once more and now (step 4) fluorescently marked primers from sPCR (green) bind to block three of msp-2. Taq-Polymerase begins amplification and thereby, block three of msp-2 is amplified. This principle is applied to both 3D7 and D10 type alleles as primers for both families are used in nested PCR.

2.2.7 Nested PCR: primary polymerase chain reaction

After DNA extraction, I used a primary polymerase chain reaction (PCR) to amplify a fragment from block 3 of the msp-2 gene. All primers were identical to the primers reported by Falk *et al.* (2006). All primers were set up for 100 pmol / µl.

The dNTP-Set was mixed using equal amounts of deoxyadenosine, deoxythymidine, deoxycytidine and deoxyguanosine. To prevent contamination, I formulated the mastermix (Table 11) in a second, malaria-naive laboratory. Here, I worked underneath a flow hood that was ultraviolet-irradiated after usage and kept my agents on an iced tablet. I first pipetted H_2O into a sterile tube. Then, I added 10 X buffer, $MgCl_2$, dNTPs 2 mM, primer S2 10 mM, primer S3 10 mM and finally the frozen *Taq*-polymerase. All agents can be seen in Table 11. I vortexed this mastermix and distributed it into PCR SingleCap 8er- SoftStrips 0.2 ml tubes with 45 µl of mastermix each.

Table 11: Agents for mastermix of pPCR.

Agent	**Amount in µl**
H_2O	31.25
10 X buffer	5.0
$MgCl_2$	3.0
dNTP Mix 2mM	5.0
Primer S2 10 mM	0.25
Primer S3 10 mM	0.25
Taq-polymerase	0.15

I added two positive controls containing a D10-type allele and a 3D7-type allele and two negative controls: the first one containing the DNA-free extraction water, the second one containing the pPCR-mastermix without DNA. I pipetted 5 µl of each extracted DNA into all other tubes and placed them into the cycler. The cycler was programmed as listed in Table 12.

Table 12: Cycler's programming for pPCR. No. stands for number.

No. of cycles	Time (in minutes)	Temperature
1	5:00	94 °C
30	0:30	94 °C
	2:00	55 °C
	2:00	70 °C
1	7:00	72 °C
		4 °C

2.2.8 Nested PCR: secondary polymerase chain reaction

The following agents were needed for the mastermix of the secondary PCR (sPCR):

Table 13: Agents for mastermix of sPCR.

Reagent	Amount in µl per sample
H_20	31.6
10 X buffer	5.0
$MgCl_2$	3.0
dNTP Mix 2mM	5.0
Primer S1 10mM	2.0
Primer M5 10mM	1.0
Primer N5 10mM	1.0
Taq	0.4

The fluorence-labeled primers M5 and N5 were stored in the dark to ensure conservation. I mixed the mastermix for the sPCR in the second, malaria-naive laboratory underneath a flow hood, which was ultraviolet-irradiated after usage, and assorted my agents on an iced tablet. To produce the sPCR-mastermix, I added H_2O, 10 X buffer, $MgCl_2$, dNTP 2mM, primer S1, labeled primers M5 and N5 and *Taq* as listed in Table 13. I vortexed the sPCR-mastermix and distributed it into PCR SingleCap 8er-SoftStrips 0.2 ml with 49 µl of mastermix. I added one new negative control with sPCR-mastermix and closed this tube's lid at once. Back in the lab, I added 1 µl of the

pPCR-amplificates each to the tubes containing the sPCR-mastermix. I shut the tubes and put them into the cycler starting the program listed in Table 14.

Table 14: Cycler's programming for sPCR.

No. of cycles	Time (in minutes)	Temperature
1	2:00	94 °C
44	0:30	94 °C
	0:45	50 °C
	1:30	70 °C
1	10:00	70 °C
		4 °C

2.2.9 Agarose gel electrophoresis

A 1.5 % agarose gel electrophoresis was assembled to determine whether DNA was successfully amplified. The agarose gel forms a matrix in which amplified, negatively charged DNA fragments can be separated by size by use of an electric field. By exposure to ultraviolet light, bands can be visualized and compared to an added size standard (so called, DNA ladder), which enables the investigator to estimate the size of DNA fragments.

Preparation:

- SYBRGreen® I 2 x 500 µl was diluted 1:100 in dimethylsulfoxide underneath a flow hood and portioned into small aliquots to inhibit a loss of function due to frequent freeze-thawing. The portions were stored at - 20 °C.
- The blue loading buffer was prepared with 0.1 g bromphenolblue, 0.1 g xylencyanol, 40 g glycerol, 2 ml 0.5 M EDTA on 100 ml H_2O and stored at 4 °C.
- The base pair size standard was prepared with 10 µl 100 bp DNA ladder, 70 µl H_2O and 20 µl of blue loading buffer.
- Orange G loading buffer was prepared with 20 ml glycerol, 0.01 g Orange G and 1 ml 500 mM EDTA.

- The 1 X TBE buffer was prepared with 216 g TRIS, 14.88 g EDTA and 111.2 g boric acid and dissolved into 2 l of deionized water. 10 X TBE buffer was assembled by diluting 1 X buffer 1:10 with deionized water.

To mix the agarose gel, I used a glass container of minimum 250 ml and 1.5 g of agarose to 100 ml of 10 X TBE buffer. A magnet mixer stirred the mixture while it boiled for several minutes in a microwave until the liquid became clear. I filled the liquid agarose gel into a tray and let it harden.

I established a loading mix by mixing 2.5 µl of blue loading mix, 1.5 µl of purified water and 1.0 µl of SYBR®Green per sample, respectively. SYBR®Green binds to double stranded DNA and serves to visualize DNA in gel electrophoresis. It emits green light at λ_{max} = 520 nm when excited with ultraviolet light.

Table 15: Loading mix.

Reagent	**Amount in µl**
Blue loading buffer	2.5
Bidest Water	1.5
SYBR®Green	1.0

I placed the hardened agarose gel into a buffer solution and pipetted 3.5 µl of size standard and 1 µl of SYBR®Green into the first pouch of the gel. I filled the other pouches with 5 µl of loading-mix and 5 µl of sPCR product. Then, I applied an electric field at 100 Volt and examined the gel after 25 – 35 minutes underneath ultraviolet light.

Lanes with DNA-positive samples were recognized due to yellow bars, which appear when the agarose gel is excited by ultraviolet light (Figure 8). These DNA-positive samples were then examined through CE and the resulting data can be inspected by the GeneMapper® software as electropherograms. In lanes with DNA-negative samples no yellow bar appeared when excited by ultraviolet light. These DNA-negative samples were examined a second time in an agarose gel using 3 µl of sPCR amplification-product. Figure 8 illustrates an agarose gel, which shows the DNA ladder in lane one, different intensities and quantities of bars in lanes two to seven and no bar in lane eight meaning that no, or very little PCR product, was visible in lane eight.

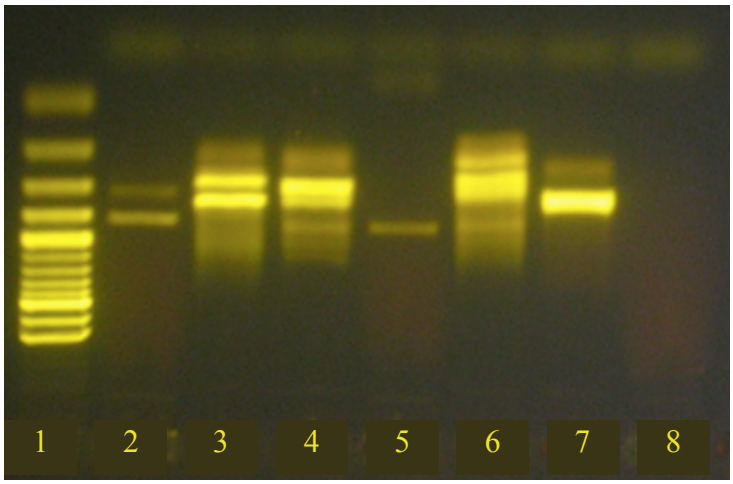

Figure 8: Fluorescenct bands in agarose gel. It is well demonstrated how the DNA size standard in lane one spreads into different bands. Each band stands for a differently sized DNA fragment. In lane five, one single band can be seen, whereas in lane two, three, four, six and seven, several bands are visible. No band and therefore no DNA shows in lane eight.

2.2.10 Capillary electrophoresis

Capillary electrophoresis (CE) is performed in form of a modified Sanger sequencing method: After having conducted pPCR, the resulting DNA fragments were marked by fluorescent dye due to fluorescently marked primers in sPCR. These fragments were then separated in a separation matrix (3130 POP-7™ Performance Optimized Polymer) within fine capillaries by an automated DNA sequencer (3130xl Genetic Analyzers, Applied Biosystems). Their sizes in base pairs (bp) were estimated by comparing the migration time of the analysed fragment with the migration time of an internal fluorescent size standard (ROX-500). The fragments and the size standard were made visible by excitation with a laser. The allele-types 3D7 and D10 were distinguished because two differently coloured allelic-type-specific fluorescent dyes were used for sPCR to label one primer per family-specific primer pair. A dedicated software (GeneMapper®) analysed the information containing both fragment size and affiliation to either 3D7 or D10 and displayed it in form of electropherograms (Liljander et al. 2009).

I performed CE only on samples that had shown a DNA-positive bar in agarose gel electrophoresis. Hi-Di™ was portioned into parts of 500 µl and frozen beforehand. I diluted the sPCR product with DNA-free water (LiChrosolv®) 1:400 at first. Then, I

pipetted 10 µl fluorescent size standard ROX-500 (range 50 – 500 bp), 2.5 µl of the diluted sPCR product and at last 10 µl of HiDi™ into each pit of a 96-well sequencer plate. I centrifuged the 96-well-plate to remove air bubbles and put the plate into its attachment. I placed it in the sequencer and chose the GeneScan® program for capillary electrophoresis. If the capillary electrophoresis did not detect any fragments, I diluted the sPCR product consecutively 1:200, 1:40, 1:5 and 1:1 until a fragment could be detected.

2.2.11 Interpretation of electropherograms

To be able to read the data that the sequencer produces, the GeneMapper® software produced electropherograms. On the x-axis one can see the length of the DNA-fragment in base pairs (bp), on the y-axis the detected intensity in relative fluorescent units (rfu). The red peaks derive from the size standard, green peaks belong to 3D7-type alleles and blue peaks to D10-type alleles. In the program, one can select the peak and read the exact length of base pairs as well as the intensity.

Figure 9 shows one single 3D7-type (green peak) allele with a length of 326 bp and an intensity of 646 rfu.

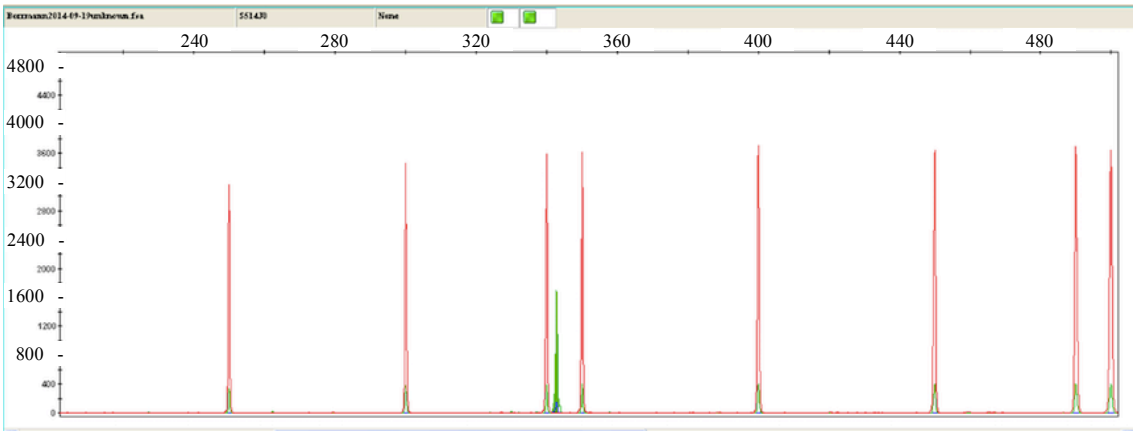

Figure 9: One single 3D7-type allele. X-axis shows length of detected PCR-fragments in bp. Y-axis depicts detected intensity in rfu.

To evaluate electropherograms with more than one peak and to decide on whether a peak can be interpreted as an allele, the cut-off was defined. The cut-off is the intensity above which a peak is interpreted as an allele. As described by Messerli *et al.* (2016), I defined the cut-off as the intensity that consists of 10 % of the highest peak.

In Figure 10 one high peak from a 3D7-type allele can be seen with a length of 276 bp and an intensity of 3480 rfu. A second peak of 344 bp must not be interpreted as an allele because its intensity is of 310 rfu, which makes it < 10 % of the highest peak.

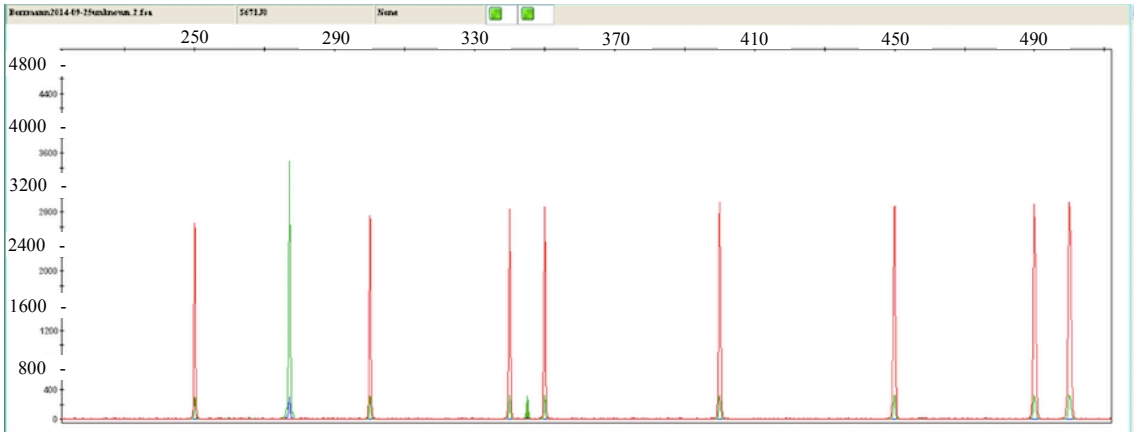

Figure 10: Two genotypes? Defining a peak. X-axis shows length of detected PCR-fragments in bp. Y-axis depicts detected intensity in rfu.

Figure 11 shows an electropherogram with six peaks of which two were counted as genotype: the highest peak D10 417 bp with an intensity of 515 rfu (blue peak) and the second highest 3D7 277 bp (green peak). The other four peaks showing an intensity of < 515 rfu were not counted genotypes.

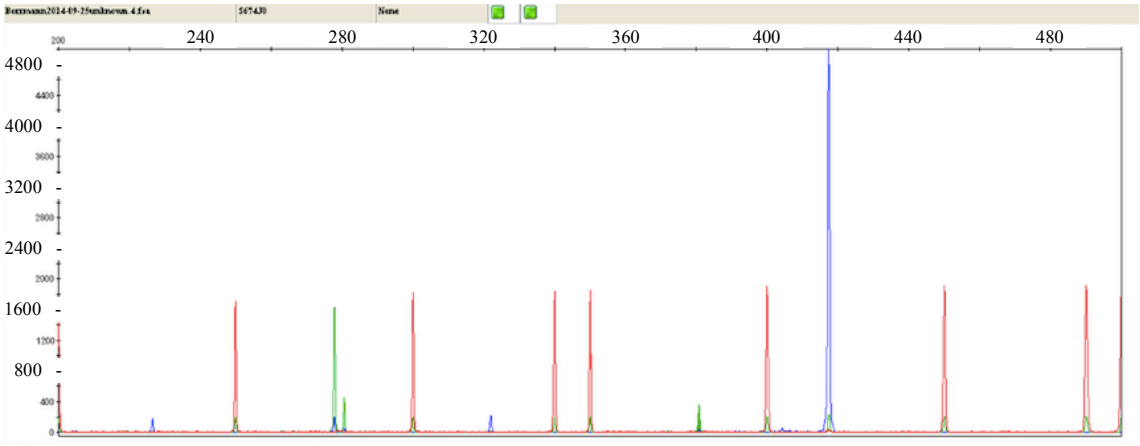

Figure 11: Several peaks. X-axis shows length of detected PCR-fragments in bp. Y-axis depicts detected intensity in rfu.

Control mechanisms

Each step during the laboratory work produced a negative control. A broad contamination would be positive in agarose gel electrophoresis by showing a band of the same size in each row. The much more precise method of CE genotyping would

show a peak at a certain fragment size in each electropherogram. An inconspicuous negative control as in Figure 12 shows the red size standard peaks but no peaks in other colours.

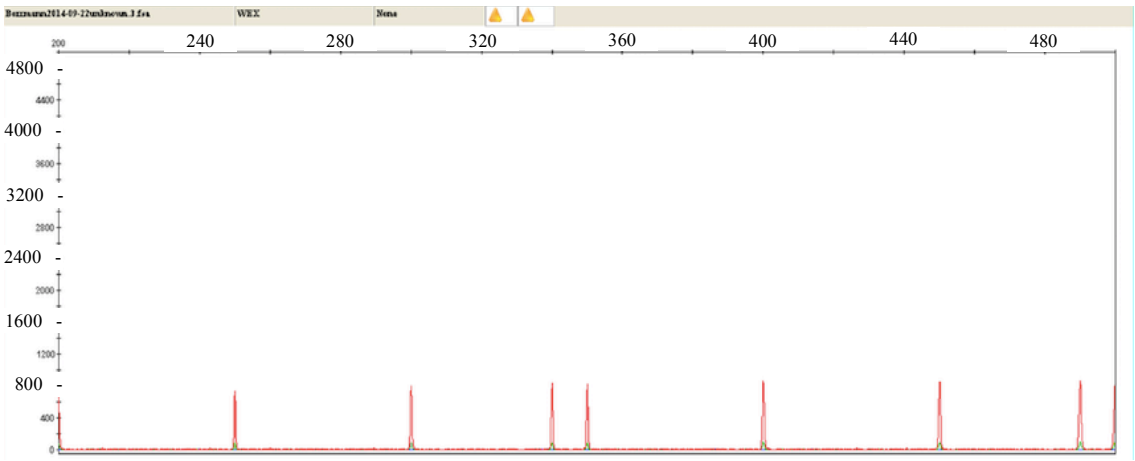

Figure 12: Inconspicuous negative control. X-axis shows length of detected PCR-fragments in bp. Y-axis depicts detected intensity in rfu.

A 3D7-type positive control with 265 bp and a D10-type positive control with 358 bp was included in the study and are shown in Figure 13 and 14.

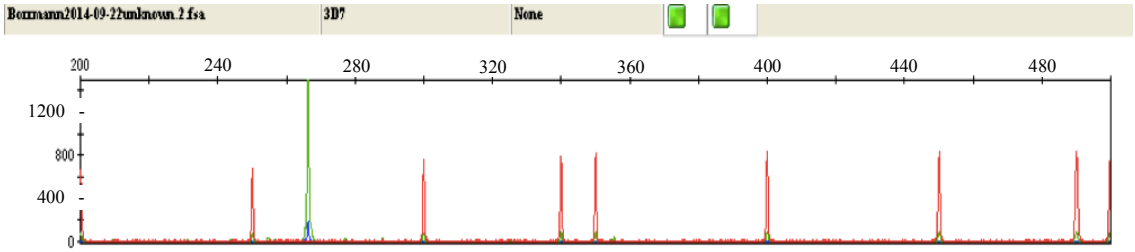

Figure 13: 3D7-type positive control. X-axis shows length of detected PCR-fragments in bp. Y-axis depicts detected intensity in rfu.

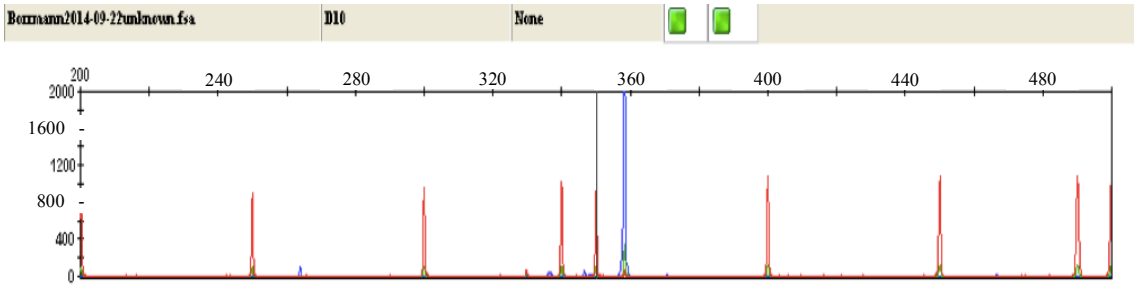

Figure 14: D10-type positive control. X-axis shows length of detected PCR-fragments in bp. Y-axis depicts detected intensity in rfu.

2.2.12 Statistical evaluation

After having noted all genotypes in an Excel table, I started the so-called process of binning. Thanks to the high sensitivity of automated CE and given that a coding region is genotyped, fragment sizes differed by multiples of 3 bp (Falk et al. 2006). I therefore manually selected 3 bp bins and evaluated recrudescence rates by comparing genotypes that had occurred in the sample at baseline (day 0) with genotypes from the samples of the day of recurrence. Furthermore, I analysed allele frequencies of the population at baseline by taking all baseline genotypes into account. The mean multiplicity of infection (MOI) was calculated as MOI = $\frac{total\ number\ of\ P.falciparum\ genotypes}{number\ of\ positive\ PCR\ samples}$ (Mwingira et al. 2011). The theoretical probability of being infected twice with the same genotype can be calculated as $P=\sum p_i^2$ with p_i being the frequency of the analysed genotype. The heterozygosity of infection (H_E) is an indicator of risk of misclassification when certain genotypes in a population occur in a high allele frequency. I calculated H_E for the genotype that appeared with the highest allele frequency as $H_E = [n/(n-1)][(1-\sum p_i^2)]$ with n = number of samples and p_i = frequency of the genotype (Schoepflin et al. 2009). I calculated the mean, median and standard deviation of selected data with a 95 % confidence interval (CI) using Excel. I used GraphPad PRISM® 7 to build descriptive graphs.

3 Results

The following chapter is divided into five parts: First, I will display a flow chart as well as examples for recurrences and reinfections on electropherograms. Then, I will present baseline characteristics of the investigated patients. I will discuss allele frequencies in the baseline population and then, I will focus on recurrences. Finally, I will present results on the mean multiplicity of infection and the heterozygosity of infection.

3.1 Implementing msp-2 genotyping of 63 paired samples from Bobo-Dioulasso

As can be seen in Figure 15 I analysed 126 samples corresponding to 63 pairs of isolates from baseline (day 0) that were retrieved before the administration of medication and from the day of asexual parasite recurrence. 47 (74.60 %) were successfully amplified. The data, which is analysed and discussed below derives therefore from these successfully amplified 47 paired samples.

The paired samples contain one baseline sample (day 0) that was retrieved before the administration of medication and one sample from the day of recurrence. 16 paired samples could not be successfully amplified. Even after multiple attempts of re-extracting DNA, amplifying and genotyping, no PCR product could be detected in the agarose gel electrophoresis. Two of the positive paired samples were excluded due to stutter peaks.

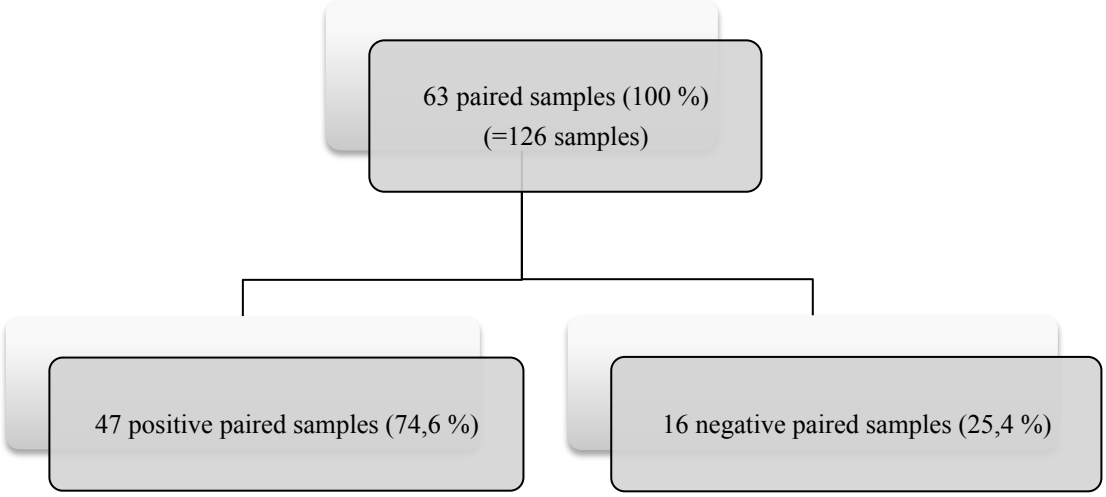

Figure 15: Flow chart demonstrating amount of positive and negative samples.

I will use the following examples for illustrating the type of data obtained and how the data were interpreted for classifying recurrent infections into either recrudescent infections (i.e., infections that appeared to persist despite treatment) or new, secondary infections. Figure 16 and Figure 17 show an example for a sample pair that represents a new infection. Each electropherogram shows a different genotype. The baseline electropherogram of day 0 shows the genotype 3D7 241 bp, whereas the electropherogram of the day of recurrence shows a genotype of 3D7 268 bp. Both peaks represent 3D7-type alleles as the colour of the peaks is green.

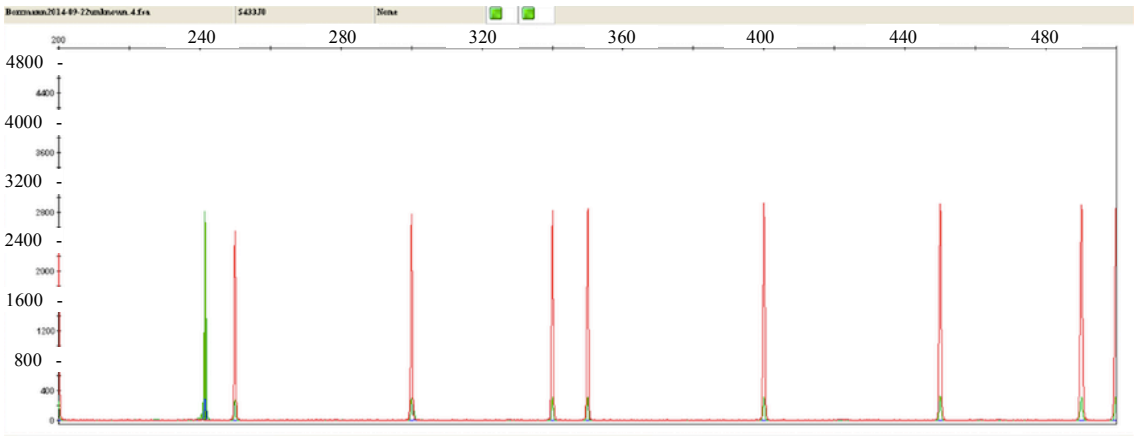

Figure 16: New infection - day 0. X-axis shows length of detected PCR-fragment in bp. Y-axis depicts detected intensity in rfu.

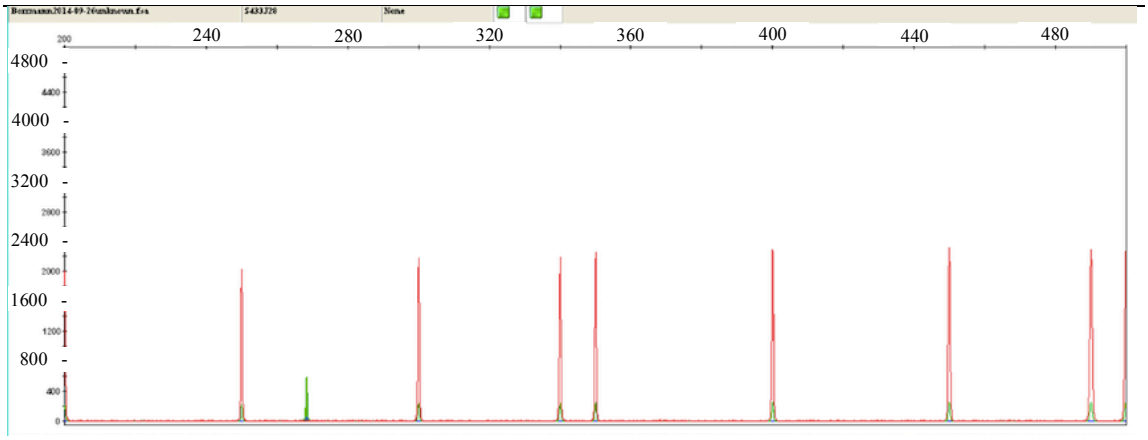

Figure 17: New infection - day of recurrence. X-axis shows length of detected PCR-fragment in bp. Y-axis depicts detected intensity in rfu.

Figure 18 and Figure 19 on the other hand demonstrate an example for a recrudescence. The electropherogram from baseline in Figure 18 shows a co-infection of two different genotypes: D10 336 bp (blue) and 3D7 272 bp (green).

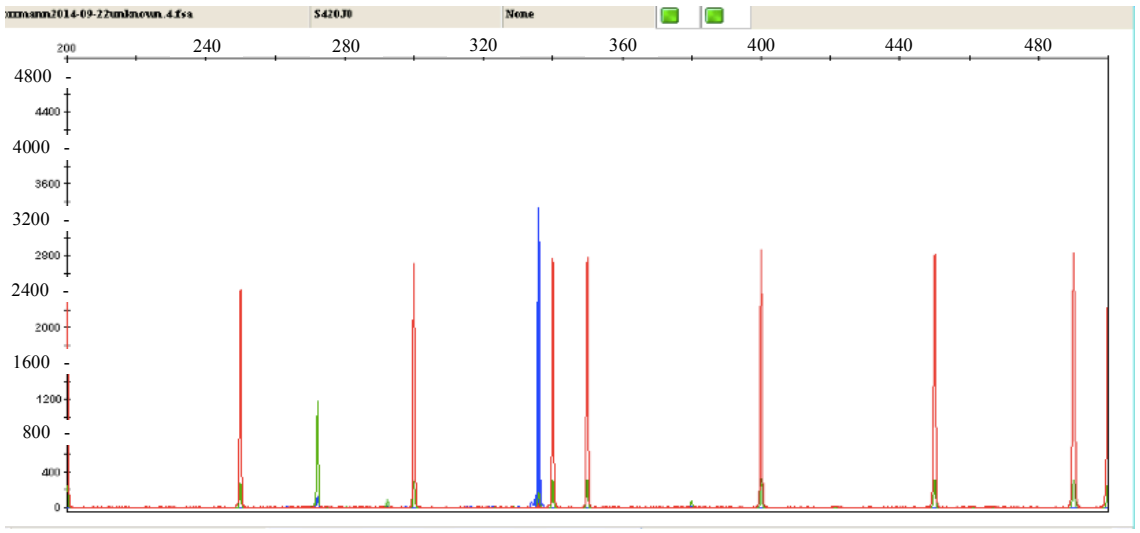

Figure 18: Recrudescence-pair: day 0. X-axis shows length of detected PCR-fragments in bp. Y-axis depicts detected intensity in rfu.

The day of recurrence in Figure 19 indicates a recrudescence due to the persistence of genotype D10 336 bp (blue peak). Additionally, a co-infection with new genotypes D10 417 bp (blue) and 3D7 252 bp (green) can be seen on the day of recurrence.

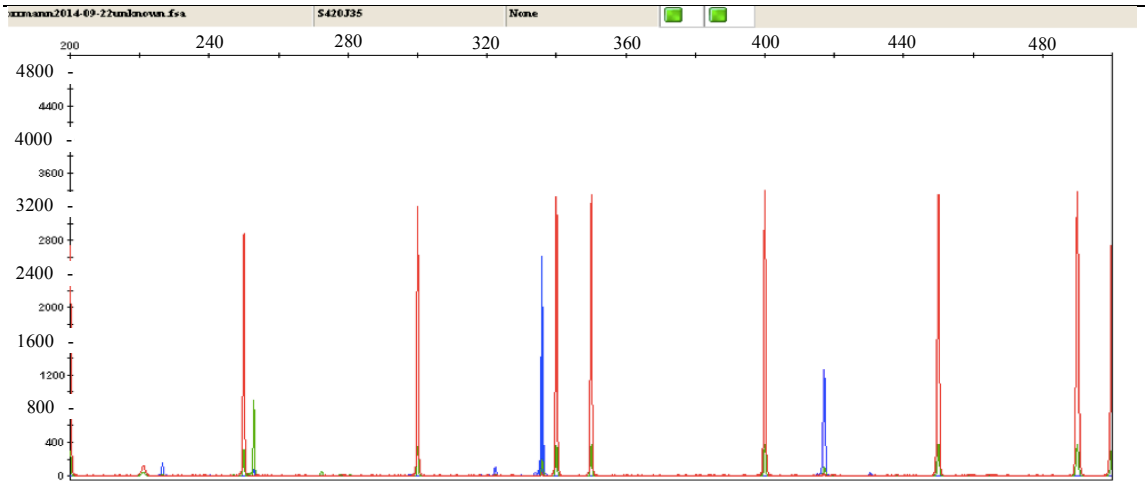

Figure 19: Recrudescence-pair: day of recurrence. X-axis shows length of detected PCR-fragments in bp. Y-axis depicts detected intensity in rfu.

3.2 Baseline characteristics

The baseline characteristics of the 47 patients are illustrated in Table 16. Due to the small sample size and the unbalanced number per treatment arm, statistical tests could not be carried out.

Table 16: Baseline characteristics of enrolled patients. SD stands for standard deviation.

Baseline characteristics	**AL** n = 36	**DP** n = 4	**PA** n = 5
Gender male / female (%)	17 / 19 (47.2) / (52.8)	3 / 1 (75) / (25)	2 / 3 (40) / (60)
Age mean (median) in years ± SD, range	7.4 (6) ± 5.7, 2 - 34	2.5 (2.5) ± 1.1, 1 – 4	6.8 (7) ± 4.3, 2 – 14
Weight mean (median) in kg ± SD	22.3 (18.7) ± 11.4	11.4 (11.6) ± 1.1	22.3 (20.9) ± 0
Parasitaemia mean (median) in µl	53 631 (28630)	75 350 (55090)	91 644 (95620)
Hemoglobin mean (median) in g / dl ± SD	10.4 (10.4) ± 1.3	9.1 (9.6) ± 1.3	10.1 (10.6) ± 1.11
Axillary temperature mean (median) in °C ± SD	37.7 (37.7) ± 1.1	38.4 (38) ± 0.8	39.1 (38.8) ± 0.6

Two patients showed gametocytaemia in their baseline sample, which in both cases disappeared before the day of recurrence. Of these two patients, one was found to have a recrudescence and one a new infection.

3.3 Allele frequency

I calculated allele frequencies by assigning all genotypes that were observed in the baseline samples by their size in base pairs into 3 bp sized "bins". (E.g., fragments of the sizes 3D7 280 bp, 281 bp and 282 bp were assigned to the bin 3D7 281 bp.) Then, I calculated the frequency of each genotype.

All genotypes that occur above 5 % belong to D10-type alleles

One particular question after having calculated the distribution and frequencies of genotypes was whether certain genotypes were overrepresented. An initial interesting observation was that all genotypes that occurred above 5 % in the baseline population belonged to D10-type alleles (Fig. 20).

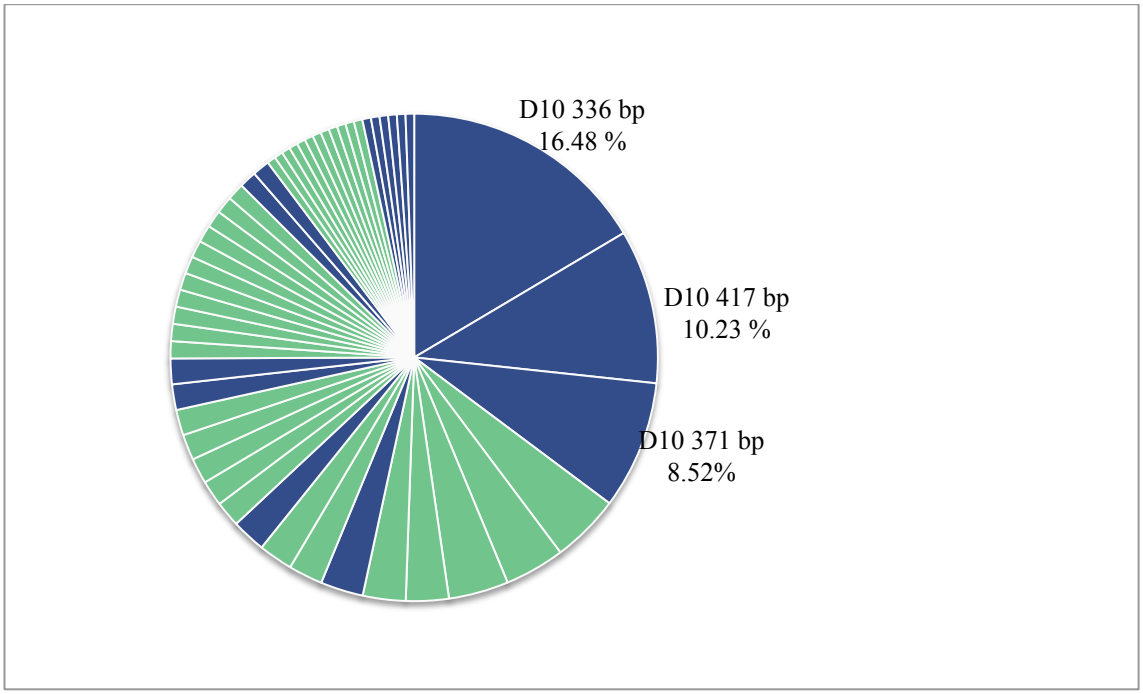

Figure 20: Allele frequency in baseline population. Frequencies > 5 % are indicated with exact allele frequency, with fragment length and allelic type. The green colour depicts 3D7-type alleles and the blue colour represents D10-type alleles. Lengths of fragment are indicated in bp.

Then, I noticed that results showed a total of 50 different genotypes being distributed between 35 3D7-type alleles and 15 D10-type alleles. However, 49.44 % of infections were caused by D10-type alleles.

When looking at allele frequencies of the two allelic families separately from one another, the polymorphic nature of 3D7 alleles with 35 alleles can be easily appreciated (Fig. 21). There is no striking frequency within 3D7-type alleles as all genotypes are represented in a certain regularity.

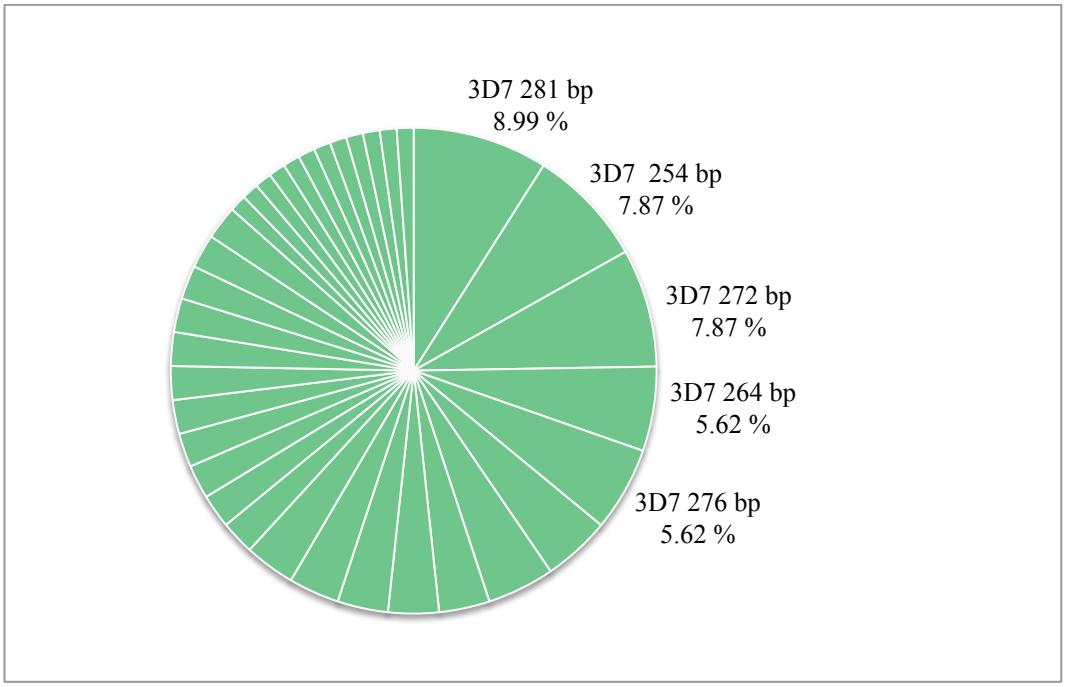

Figure 21: Allele frequencies of only 3D7-type alleles. Frequencies > 5 % are indicated with exact allele frequency, with fragment length and allelic type. The green colour depicts 3D7-type alleles. Lengths of fragment are indicated in bp.

In contrast, within the D10-type alleles, 77.01 % were represented by only four different genotypes. In particular, three genotypes with the following fragment size are overrepresented: 336 bp, 417 bp and 371 bp with 33.33 %, 20.69 % and 17.24 %, respectively. Figure 22 depicts this pattern by showing all 15 D10-type alleles and highlighting all genotypes with frequencies above 5 %.

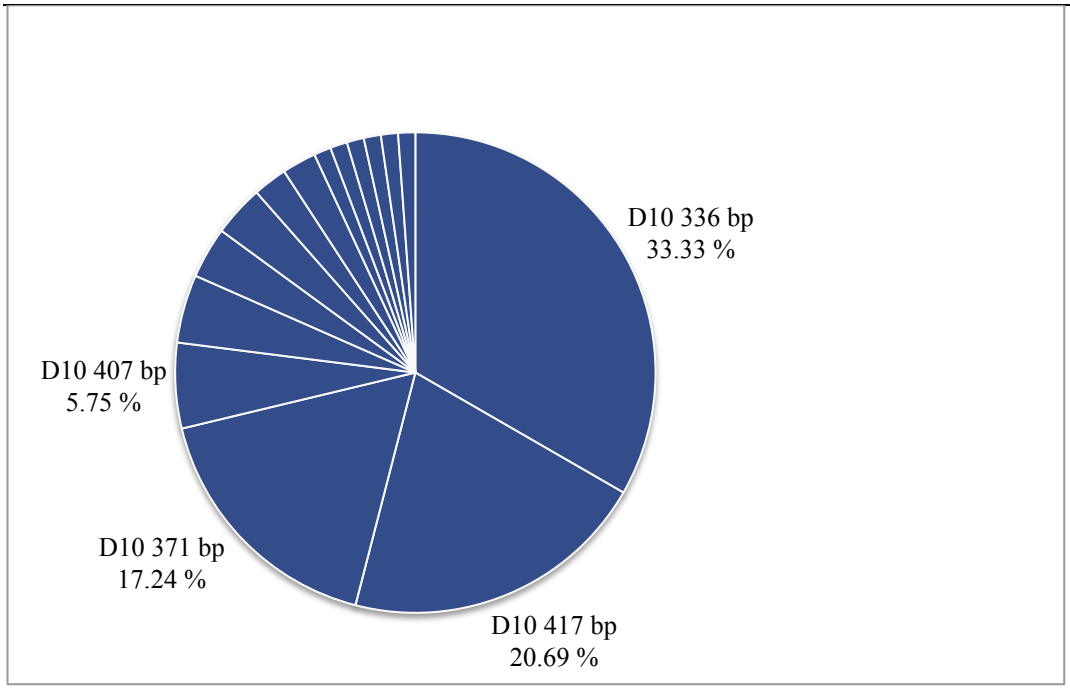

Figure 22: Allele frequencies of only D10-type alleles. Frequencies > 5 % are indicated with exact allele frequency, with fragment length and allelic type. The blue colour represents D10-type alleles. Lengths of fragment are indicated in bp.

In summary, 3D7-type alleles were more diverse than D10-type alleles. Certain D10-type alleles, however, were represented in higher frequencies. To examine the distributions once more, I constructed Figure 23 and Figure 24. Figure 23 shows that 3D7-type alleles have a slightly skewed distribution over a wide range of fragment lengths. In stark contrast, D10-type alleles (Fig. 24) exhibit a pronounced discrete distribution pattern – three alleles across the range of observed fragment lengths are clearly dominant.

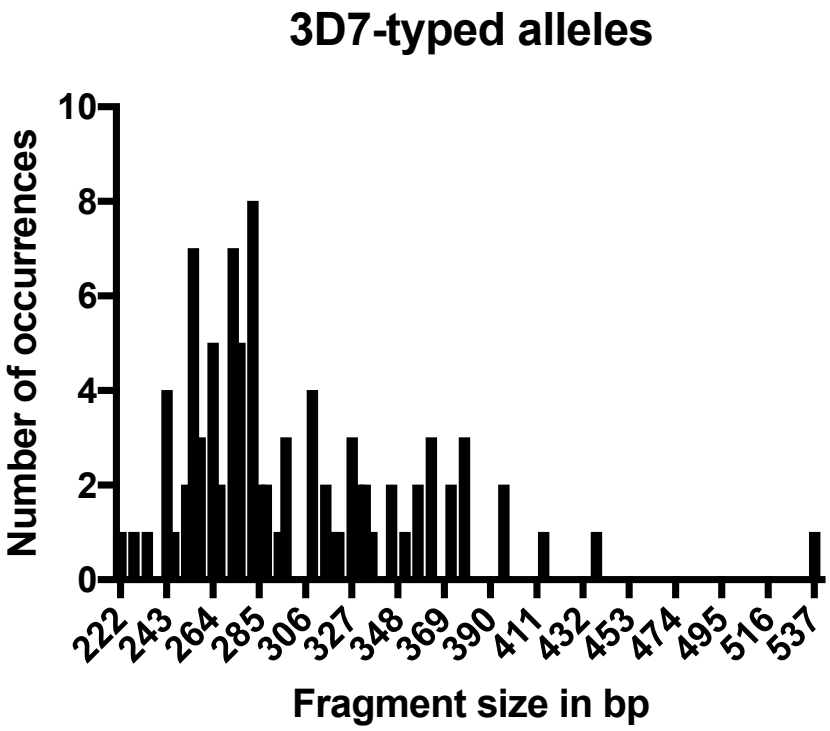

Figure 23: Fragment sizes and respective frequency of 3D7-type alleles. X-axis showing fragment size in bp, y-axis demonstrating the number of occurrences.

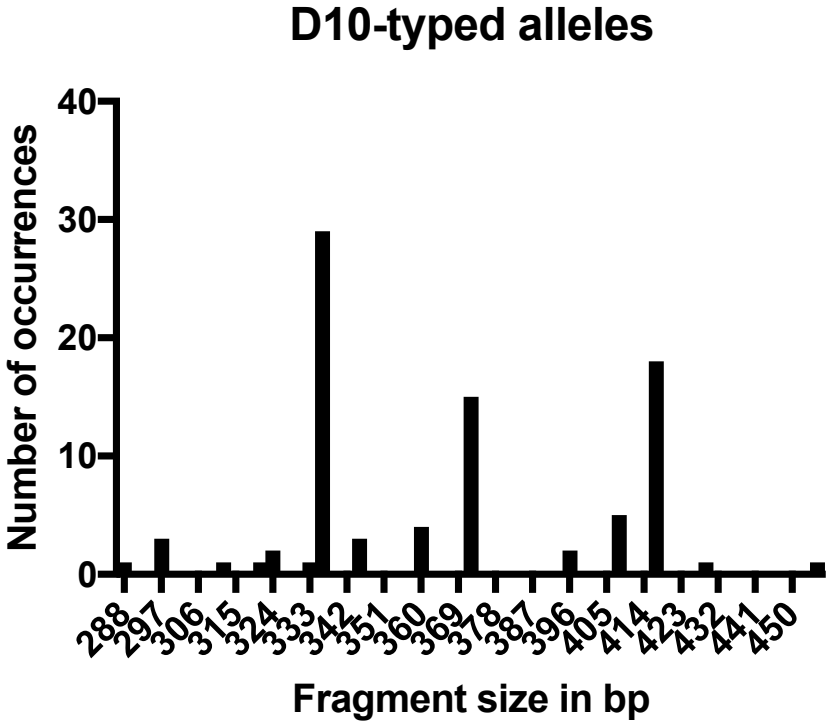

Figure 24: Fragment sizes and respective frequency of D10-type alleles. X-axis showing fragment size in bp, y-axis demonstrating the number of occurrences.

Concluding the analysis of allele frequencies among baseline samples, it can be said that firstly, all genotypes that occurred > 5 % in the baseline population belonged to D10-type alleles and secondly, 3D7-type alleles were far more diverse than D10-type alleles.

Certain genotypes, primarily D10 336 bp, is overrepresented

D10 336 bp stands out due to its high representation of 16.48 %, but also certain other genotypes stand out due to their high allele frequency. Having detected this pattern, I wondered about the reasons of the overrepresented genotypes, especially D10 336 bp, and whether a bias might have occurred.

Genotypes found in negative control

While comparing the pie charts it stands out that the dataset from Bobo-Dioulasso has one prominent genotype: D10 336 bp. I checked all negative controls to understand whether the high appearance of this genotype could be explained by a contamination. The total of negative controls was 19. Six negative controls were inconspicuous, but 12 out of 19 negative controls could not be examined successfully by CE; the GeneScan® software produced unreadable electropherograms. One negative control attracted attention because it was contaminated. Figure 25 shows an inconspicuous negative control, whereas Figure 26 illustrates the contaminated negative control.

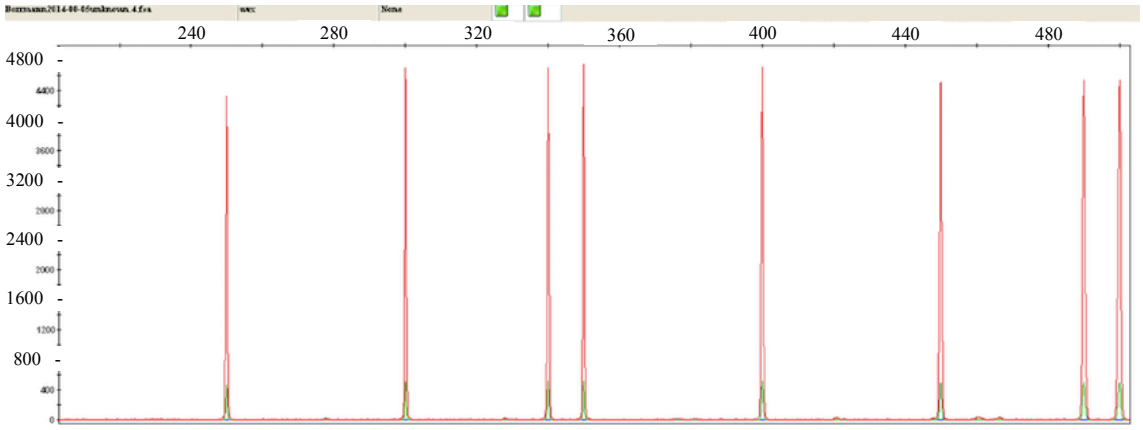

Figure 25: Inconspicuous negative control. X-axis shows length of detected PCR-fragments in bp. Y-axis depicts detected intensity in rfu.

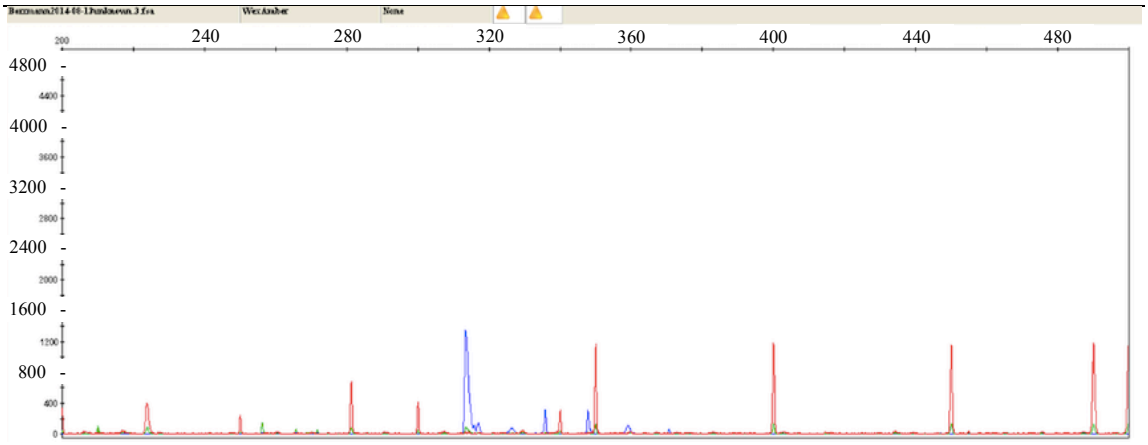

Figure 26: Contaminated negative control. X-axis shows length of detected PCR-fragments in bp. Y-axis depicts detected intensity in rfu.

To analyse whether this negative control had an outcome on my results, I arranged Table 17, which illustrates the genotypes that occurred in the contaminated negative control and shows how often these genotypes appeared in the baseline population and in recrudescences. The following PCR-fragments are represented above cut-off and were therefore interpreted as contaminations: 3D7 254 bp, D10 313 bp, D10 336 bp and D10 348 bp.

Table 17 Genotypes detected in contaminated negative control and their frequency in the baseline population.

	Size (bp)	**Baseline population (%)**
3D7	**254**	3.98
D10	**313**	0.57
	336	16.48
	348	-

Three out of four genotypes appeared in the baseline population in different frequencies.

Repeating CE genotyping led to consisting results

As an attempt to double-check whether the results that I gained during my laboratory work contained errors, a second analysis of the samples was undertaken two years after the first analysis. In the following, the first analysis that I conducted will be referred as Genotyping-2014 and the second analysis will be referred as Genotyping-2016.

In Genotyping-2016, only 44 of 126 samples (34.92 %) could be evaluated. Out of these 44 samples, 28 samples showed identical genotypes and 16 samples revealed identical genotypes but additional genotypes in Genotyping-2014.

These results from 2016 confirm the results from 2014 and therefore a contamination in the step of PCR or CE is unlikely. However, given that a new DNA extraction from filter paper blood samples was not consistently possible due to a lack of samples, Genotyping-2016 was conducted using previously extracted DNA from the laboratory work in 2014. It can thereby not be excluded that a contamination in the first step of genotyping, the DNA extraction, had occurred.

For the reason of possible bias, I decided to exclude the genotypes from the contaminated negative control and to recalculate the allele frequencies. For all further calculations, the genotypes listed in Table 17 were excluded.

Excluding genotypes

By excluding all genotypes listed in Table 17, certain paired samples, which had only shown one of the genotypes from the contaminated negative control and no other genotypes, were excluded from further analysis.

Out of 63 paired samples, 47 could be extracted and amplified. Two paired samples within the AL-arm were excluded due to stutter peaks. 16 paired samples could not be successfully extracted or amplified; three complete paired samples (2 AL, 1 DP) could not be examined as well as 13 single samples (12 AL, 1 DP). If a single sample could not be extracted and amplified successfully, the corresponding paired sample to which it belonged was excluded as for this analysis only fully paired samples were examined through CE genotyping. Thus, the sample size consisted of 37 paired samples for all further calculations (Fig. 27). I recalculated allele frequencies with all genotypes from these 37 sample pairs.

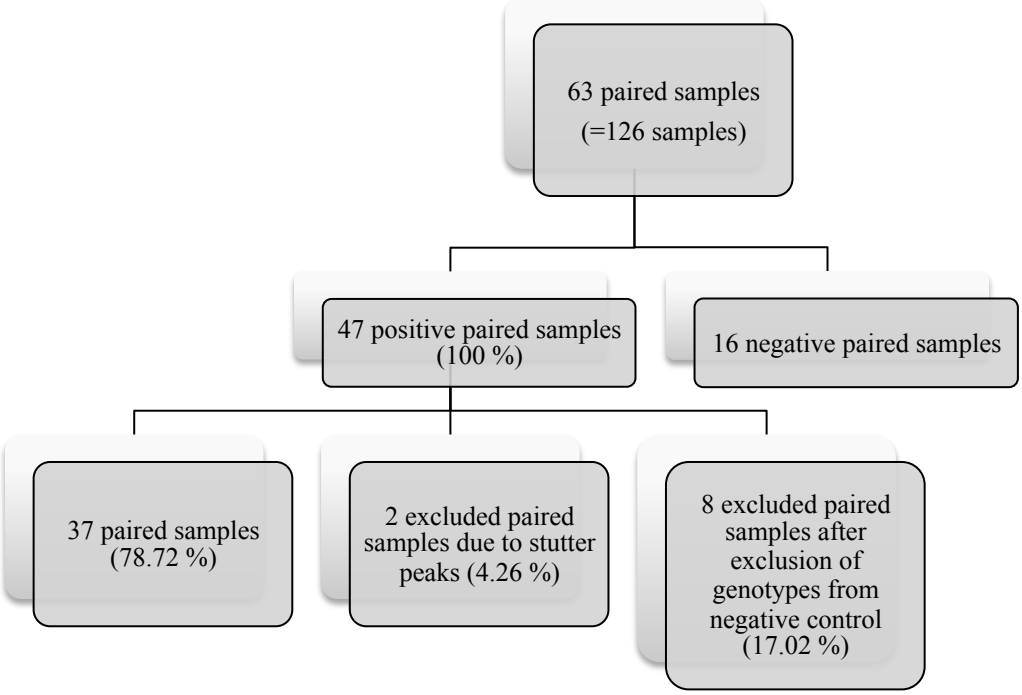

Figure 27: Positive and negative samples demonstrating amount of analysed and excluded samples.

It can be seen in Figure 28 that after excluding the genotype D10 336, other D10 genotypes are overrepresented. In spite of having excluded possibly biasing genotypes, D10 genotypes are represented in a small variable of genotypes, but in high allele frequencies, as could be shown before. 3D7 genotypes on the other hand are represented in a polymorphic pattern with frequencies of 5.61 % or lower. Figures 29 to 30 illustrate these findings.

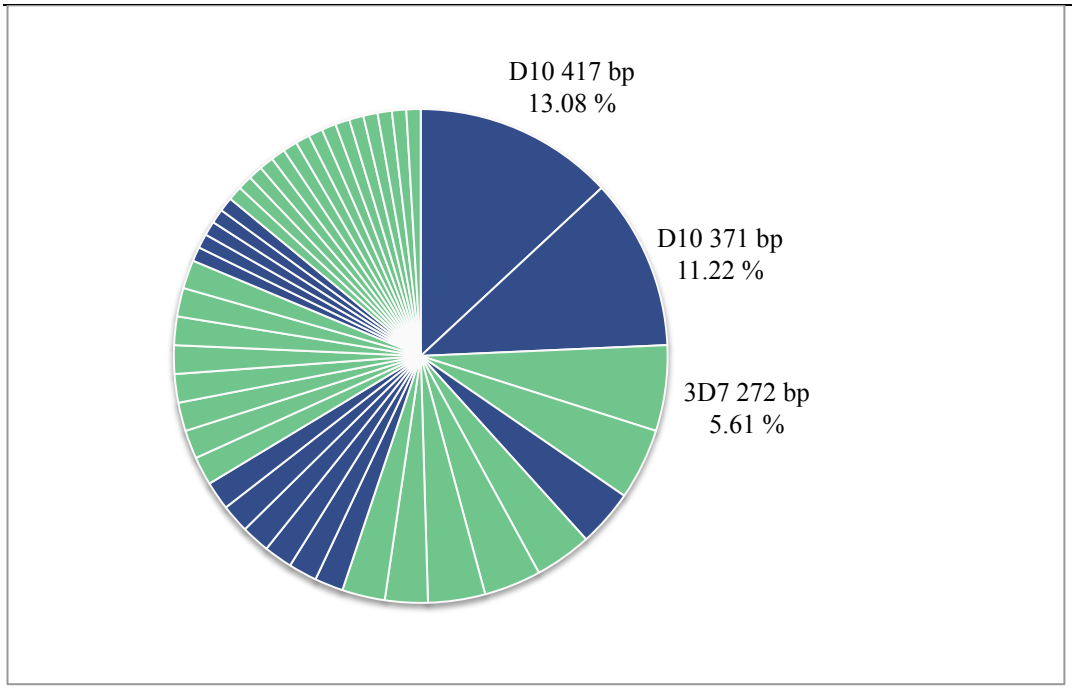

Figure 28: Allele frequency without excluded genotypes. Frequencies > 5 % are indicated with exact allele frequency, with fragment length and allelic type. The green colour depicts 3D7-type alleles and the blue colour represents D10-type alleles. Lengths of fragment are indicated in bp.

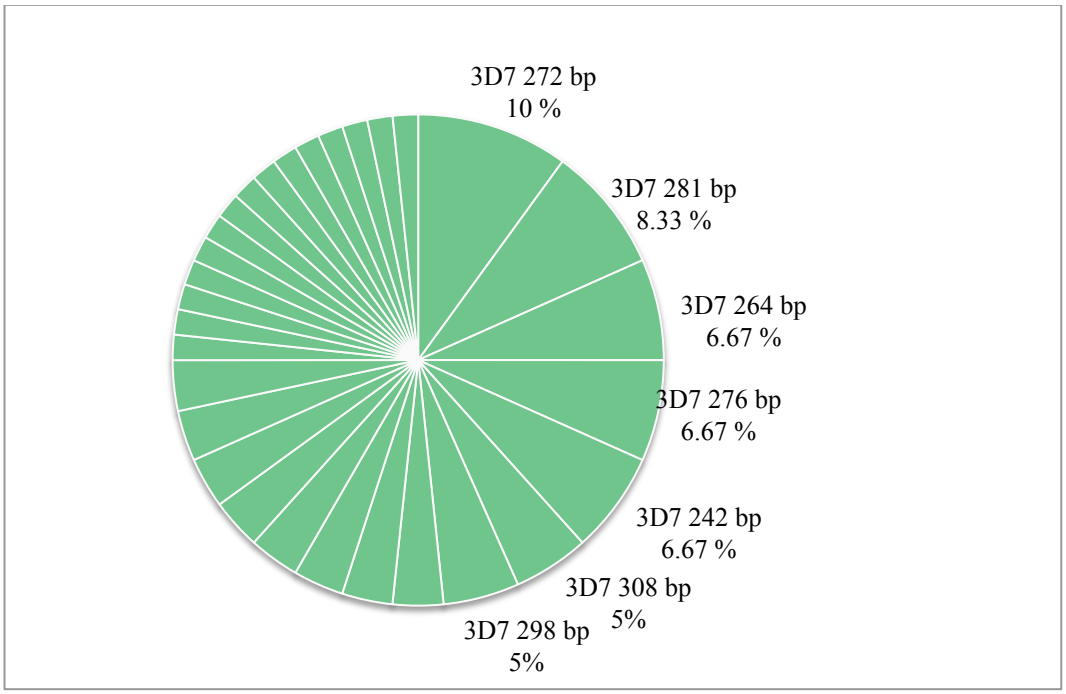

Figure 29: Only 3D7-type alleles without excluded genotypes. Frequencies > 5 % are indicated with exact allele frequency, with fragment length and allelic type. The green colour depicts 3D7-type alleles. Lengths of fragment are indicated in bp.

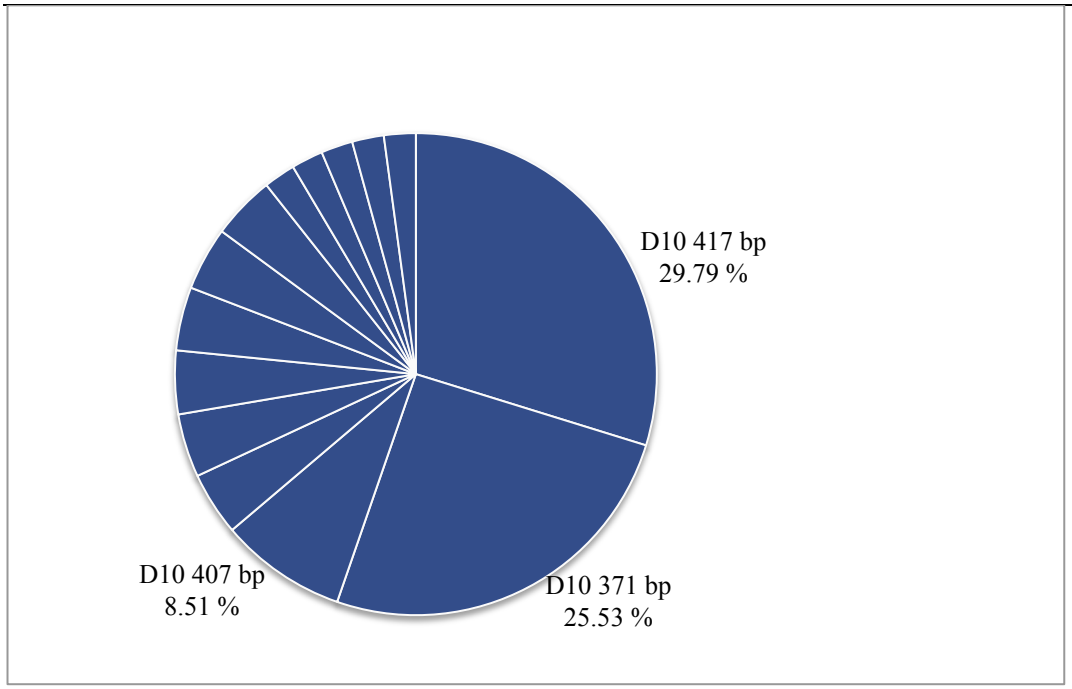

Figure 30: Only D10-type alleles without excluded genotypes. Frequencies > 5 % are indicated with exact allele frequency, with fragment length and allelic type. The blue colour represents D10-type alleles. Lengths of fragment are indicated as bp.

3.4 Recurrences

Recrudescences per treatment arms

Given the low sample size and equally important, the uneven distribution of samples between study groups, I will use the limited available data for illustrating the power of precise genotyping for the interpretation of antimalarial drug trials.

Out of 37 paired samples, 29 paired samples belonged to the AL-treatment arm, and 4 to the DP and the PA-treatment arm, respectively (Fig. 31).

Figure 32 further depicts how many recurrences, meaning the sum of new infections and recrudescences, and how many recrudescences appeared in each treatment arm: seven recrudescences in the AL treatment arm and one recrudescence in the PA treatment arm. No recrudescence appeared in de DP treatment arm. The percentage of recrudescences in my small sample size was of 21.62 %. 24.14 % of samples from the AL treatment arm and 25 % of samples in the PA treatment arm showed recrudescences.

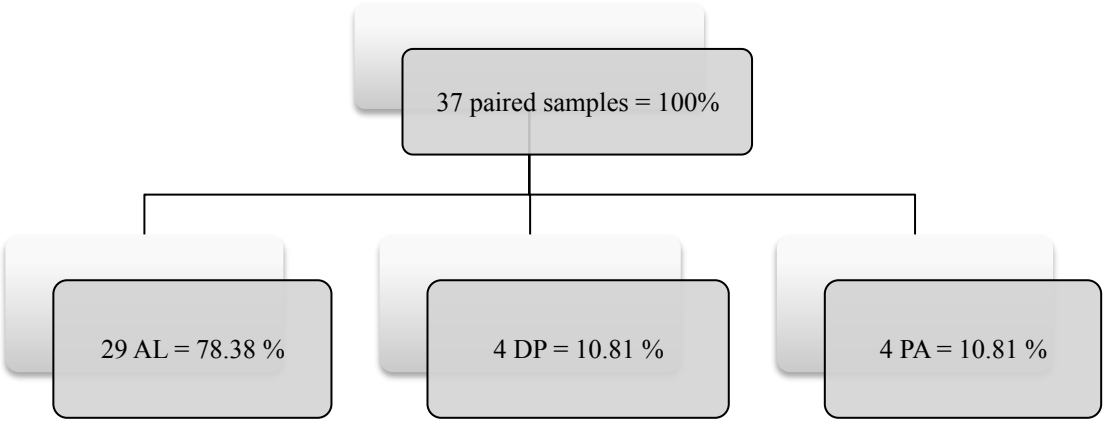

Figure 31: Analysed samples. Distribution per treatment arm.

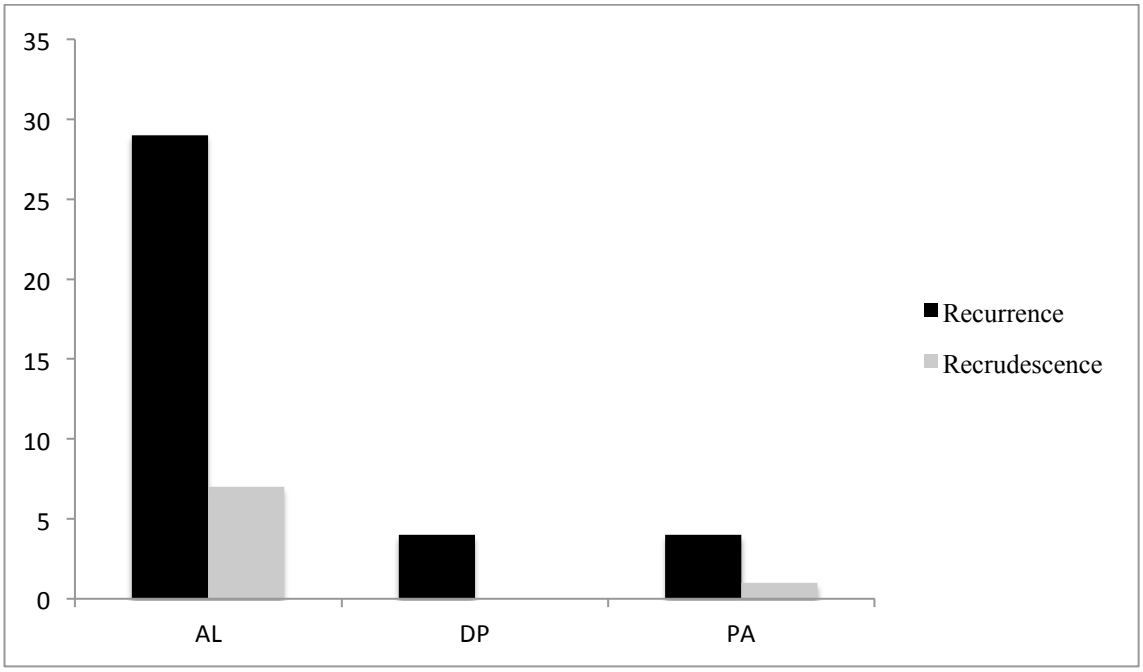

Figure 32: Amount of recurrences (black), hence the sum of new infections and recrudescences, compared to amount of recrudescences (gray) distributed by allocated treatment arm. X-axis number of paired samples. Y-axis allocation to treatment arm.

Analysing genotypes represented in recrudescences

As I analysed allele frequencies in the previous chapter, I noticed that two genotypes in particular (D10 371 bp and D10 417 bp) were overrepresented in the baseline population. The next step was to examine whether these genotypes were

overrepresented within recrudescences as well. I constructed Figure 33 to examine the distribution of genotypes among recrudescences.

Recrudescences appeared in 8 cases. Figure 33 underlines our findings from above: Fewer D10 genotypes are highly represented, and 3D7 is represented in a higher variety. For D10 genotypes, the two genotypes with the highest allele frequencies in the baseline population (D10 417 bp with 13.08 % and D10 371 bp with 11.22 %) are represented with two (25 %) recrudescences each. In the baseline population, the four 3D7 genotypes, which are responsible for recrudescences, are represented with a frequency of 1.87 % (3D7 326 bp) and 3.74 % (3D7 242 bp, 3D7 264 bp, 3D7 276 bp). In recrudescences they hold a frequency of 12.5 %. Even though other 3D7 genotypes are represented in the baseline population with up to 5.61 % (3D7 272 bp), the latter are not proportionally represented in recrudescences. This means, that not only the frequency in the baseline population has an impact on its representation in recrudescences. It should be concerned that certain genotypes hold more dominance than others. It has to be said, though, that the data represented in this thesis is limited due to its small sample size and uneven distribution between treatment arms. Further analyses from a bigger sample size have to be awaited before drawing conclusions.

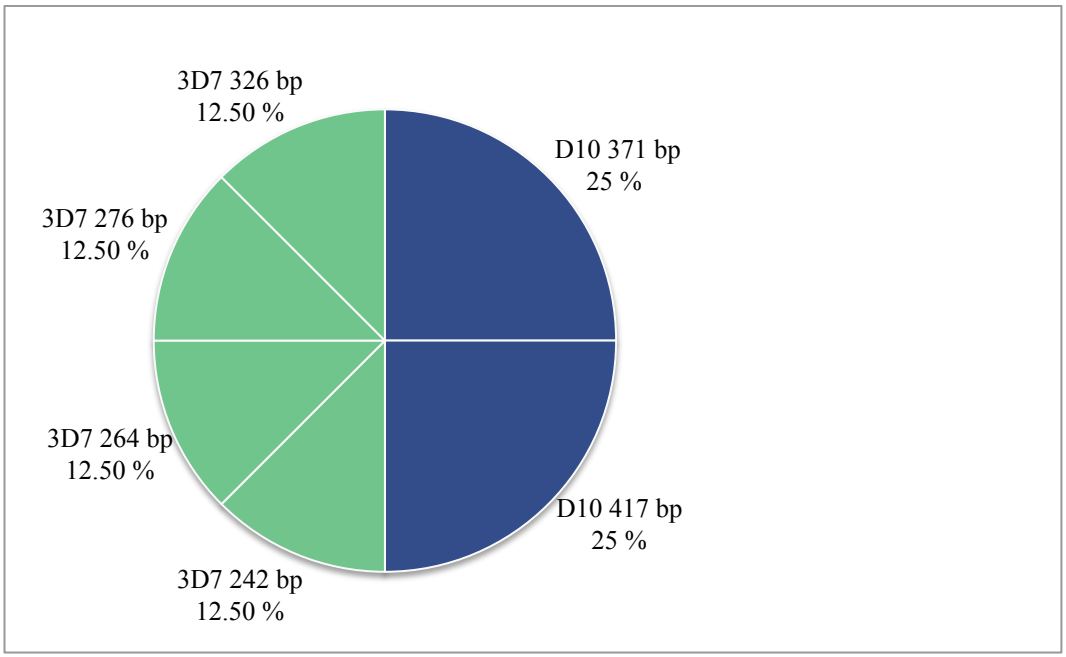

Figure 33: Genotypes in recrudescences. The genotypes are depicted in their respective frequencies and fragment length. Green colour represents 3D7-type alleles and blue colour depicts D10-type alleles. Lengths of fragment are indicated as bp.

3.5 MOI, P and heterozygosity of infection

Risk of falsely classified recrudescence due to high frequency

A misclassification as a recrudescence may occur, when in reality the recurrence is caused by a second infection with the same genotype. I calculated the probability of being infected twice by two different parasites with an identical genotype. I did this by putting the frequency in the baseline population by the power of two. It becomes clear that even in genotypes, which appeared in a high allele frequency in the studied dataset, the probability of being infected by two parasites with the same genotype is very low and thus, it is unlikely that a recurrence showing a recrudescence derives from a second infection with the same genotype. I constructed Table 18 to demonstrate the frequency of recrudescent genotypes and to compare it to the frequency in the baseline population. Furthermore, it depicts the probability of being infected twice by a parasite with an identical genotype for all genotypes that occurred in recrudescences. Even genotypes with a frequency of 25 % in recrudescences showed only a probability of 1.26 % of a second infection with a parasite holding the same genotype. This source of bias can therefore be neglected for the examined population.

Table 18 Genotypes in recrudescences. Their frequency in the baseline population and in recrudescences. Moreover, the probability of being infected by two parasites with the same genotype for each genotype.

Genotype	Allele frequency in baseline population	Frequency in recrudescence	Probability of being infected by two parasites with same genotype
D10 371 bp	0.1122	0.25	0.0126
D10 417 bp	0.1308	0.25	0.0171
3D7 242 bp	0.0374	0.125	0.0014
3D7 264 bp	0.0374	0.125	0.0014
3D7 276 bp	0.0374	0.125	0.0014
3D7 326 bp	0.0187	0.125	0.0003

MOI and HE correspond to expected values in a high transmission area

High allele frequencies in an investigated population can be the cause for misclassification of recrudescences: when certain allele frequencies are very high, the probability increases of being re-infected by chance a second time with the same genotype. This would lead to misclassifications as recrudescences when in reality it is a new infection with the same genotype. CE genotyping cannot distinguish between this incidence and a real recrudescence, but the below specified parameters formulate an approach to understand the probability of real recrudescences. Furthermore, they are a measure for genetic diversity of the population as much as a possability to assess the discriminatory power of the msp-2 marker. The formulas for MOI, P and for H_E are specified in chapter 2.2.12.

The MOI is an indicator for the transmission intensity in an examined population. High MOI is typical for high transmission areas and implies than an infection is likely to be caused by more than one genotype. In this thesis the MOI was calculated as MOI = 2.89.

The theoretical probability P of being re-infected a second time by an identical genotype is calculated to understand whether the marker gene used for CE genotyping is polymorphic enough for showing adequate discrimination power. In this thesis, msp-2 was chosen as marker gene as it is known for its polymorphic nature. P stands for the theoretical probability of being infected two times by two different parasites sharing the same genotype. For this dataset, I calculated P = 0.0486.

H_E was calculated to understand the probability that two alleles, which were randomly selected from all samples, are different. H_E is defined as the probability of two randomly selected genotypes are different in the population and was calculated as $H_E = 0.978$ for the study at hand.

3.6 Summary

I calculated allele frequencies and recrudescences. Analysing my results demonstrated several findings on characteristics of 3D7-type alleles compared to D10-type alleles. 3D7-type alleles occur with a higher polymorphism, but D10-type alleles occur in

higher frequencies, both in the baseline population and in recrudescences. I calculated recrudescence rates per treatment arm and analysed allele frequencies in recrudescences. It was confirmed in recrudescences, that 3D7 showed a higher polymorphism and that D10 was represented in a fewer number but each genotype in a higher frequency. Last, I calculated approaches to understand the probability of falsely classified recrudescences and to measure the genetic diversity of the studied population.

The question remains why D10-type alleles often appear in high allele frequencies and why certain genotypes are overrepresented. To be able to understand whether results from the present study are compatible with findings from unpublished and published data, I analysed and compared them with my results in the following chapter.

4 Discussion

Genotyping has become an important tool to assess PCR-corrected treatment failure rates in antimalarial drug trials and therefore to investigate resistances. I conducted a study implementing a genotyping protocol with CE with an automated sequencer and analysed my samples regarding recrudescence rates and allele frequencies.

Below, I will start discussing technical limitations of the methods and limitations of genotyping due to the malaria parasite's biology. I will then put my results in a broader context and compare my results with published data and with two datasets from the CATMAP-trial, which took place in Kilifi. Finally, I will close with future prospects and conclusions drawn from my study.

4.1 Technical limitations

Each step of genotyping holds certain limitations. In the following I will discuss the limitations that I encountered during my analyses.

DNA extraction

DNA was extracted from blood samples on untreated Whatman™ 3MM collection cards even though untreated filter papers do not protect from degradation of nucleases, oxidation, UV damage or microbial fungal growth and should be avoided for the purpose of genotyping (World Health Organization 2008). Instead, treated collection cards that guarantee a high quality of DNA storage should be used (Felger & Snounou 2008). However, untreated collection cards are available at low cost and are therefore frequently used in field studies.

The volume of blood size is crucial when it comes to genotyping; too small volumes may result in a negative result in spite of peripheral parasitaemia. However, collecting blood samples on filter papers leads to non-standardized blood volumes and it is difficult to estimate the amount of blood on the collection cards. Within the samples for this study the amount of blood on the filter paper varied visibly.

DNA extraction was not performed with a commercial extraction kit but using the methanol method. As could be shown in this study by conducting two PCRs using the

same extracted DNA two years apart this method may not allow a long-term storage of extracted DNA. In Genotyping-2014, the amplification was conducted within a few days after extraction of DNA and was successful in 74.60 %. For Genotyping-2016, the same extracted DNA was taken two years later and only 34.92 % of samples could be successfully amplified. Moreover, 28 samples showed additional genotypes in Genotyping-2014 compared to Genotyping-2016 indicating that DNA may have denatured in the mean time. A review by Collins *et al.* (2006) states that only 1 % of the analysed studies used the methanol method to extract DNA and rather suggests using the Chelex method if not extraction kits.

PCR

A typical problem of PCR is a defective *Taq*-polymerase. This may happen due to frequent freeze thawing (Felger & Snounou 2008) or when *Taq*-polymerase loses its activity before the reaction should start because it has thawed too early. To prevent this, on the one hand I portioned the *Taq*-polymerase into small aliquots to avoid frequent freeze thawing of each aliquot. On the other hand I worked on an iced tablet and pipetted the *Taq*-polymerase as last agent into the mastermix to prevent early onset of loss of activity.

Moreover, using the fitting primer is essential to have a productive outcome. The M5 and N5 primers for the sPCR are marked by a fluorescent tail, which loses its fluorescent activity when it encounters light. To prevent the loss of fluorescent activity, M5 and N5 were stored in opaque reservoirs.

Due to several biological reasons, which will be discussed subsequently, *P. falciparum* DNA may be represented in small quantities in the patient's blood stream. If the amount of *P. falciparum* DNA is very low, it may fall underneath the detection limit and can therefore not be examined using genotyping. Genotyping may therefore not reflect the true amount of possible coexisting infections, which may lead to a misclassification of a recurrence and therefore should be considered as possible source of error.

Positive and negative controls are crucial tools to make a statement about the credibility of a study, as PCR is susceptible for contamination. In the present study, a *P. falciparum* negative human DNA control was not established despite the suggestion by World Health Organization (2008). I introduced negative controls in each step of

genotyping and added positive controls for both allelic families. In 12 cases, negative controls were not interpretable by the GeneScan® software and could therefore not be depicted as electropherograms. To assure that no contamination has taken place, it would be of importance to be able to read the data of these not interpretable negative controls, which means that in this case it would have been appropriate to repeat the analyses on these samples. Moreover, one negative control was contaminated with four genotypes, which led to an exclusion of these genotypes and repeated calculation of allele frequencies to exclude the bias of contamination. A second genotyping procedure was conducted with the same samples that led to consisting results and confirms that no relevant contamination had appeared in during PCR. However, given that a new DNA extraction from filter paper blood samples was not consistently possible due to a lack of samples, Genotyping-2016 was conducted using previously extracted DNA from the laboratory work in 2014. It can thereby not be fully excluded that a contamination had occurred in the first step of genotyping, in the DNA extraction.

Interpretation of electropherograms

One disadvantage of CE genotyping is the interpretation of electropherograms; to be able to read electropherograms, it is of fundamental importance to determine a cut-off that defines which peaks to count as genotypes. The cut-off in the present study was defined as 0.1 rfu of the highest peak in each electropherogram as shown by Messerli *et al.* (2016). Other work groups have defined the cut-off differently: Choosing the cut-off at 300 rfu as shown by Liljander *et al.* (2009) brings the drawback of misinterpreting electropherograms. In my study, I could show that this method results in defective findings: I compared Genotyping-2014 and Genotyping-2016 and saw that in 16 cases, peaks < 300 rfu in Genotyping-2016 appeared as clear peaks above 300 rfu in Genotyping-2014. This implies that these peaks did derive from real msp-2 fragments, but that other factors caused smaller peaks underneath 300 rfu in Genotyping-2016.

A different method to define the cut-off is described by Falk *et al.* (2006), who used an in-house generated software to identify each peak by sample-specific evaluation. Not having had this possibility, I chose to determine the cut-off as described above. This method gives the possibility to consider sample-specific effects and therefore guarantees a higher standard.

Another difficulty in the interpretation of electropherograms is the appearance of artefacts such as inherent fluorescent background, which usually shows peaks below 50 rfu (Liljander et al. 2009) and can therefore easily be excluded. Stutter peaks on the other hand appear as an artefact that is explained by slipped strand mispairing (Walsh et al. 1996). Stutter peaks are characterized by regular peaks approximately every 20 bp and an intensity that is often represented by < 10 % of the highest peak in the electropherogram (Liljander et al. 2009). The example shown in Figure 34, which can be seen in the appendix, shows stutter peaks with gaps of 16 – 19 bp. Because of the difficulty of understanding with certainty whether a peak belongs to a genotype or to the stutter peak, two samples showing stutter peaks were excluded from analysis in this study.

Genetic markers

In the study at hand I introduced a protocol for msp-2 genotyping to samples from the WANECAM-trial. Before classifying a sample as a recrudescence, several steps of genotyping have to be completed: According to World Health Organization (2008) a recrudescence that was defined after having conducted genotyping with msp-2 markers has to be reinvestigated by using the GLURP marker. If genotyping with GLURP still indicates a recrudescence, msp-1 should be analysed. Only now, after having examined all three markers consecutively and after having detected a recrudescence in all three procedures, a sample can be defined as a recrudescence.

Given that for the present study only msp-2 was analysed, samples that were labelled as recrudescences should be examined with the GLURP marker and if needed with the msp-1 marker. The results of this study can therefore not lead to the assumption that the efficacy of the examined drugs is impaired before further analyses.

4.2 Biological aspects

Several biological aspects of the *P. falciparum* life cycle have to be considered when critically evaluating *P. falciparum* genotyping. These aspects include the late appearance of gametocytes long after the disappearance of asexual blood stages from the blood stream, but also the characteristics of the *P. falciparum* life cycle in the

human host. In addition, I will discuss certain aspects of transmission dynamics between the human and the anopheline host.

Gametocytes

Gametocytes derive from asexual blood stages and become detectable in the peripheral blood stream 7 – 15 days after the appearance of the latter (Bousema & Drakeley 2011). If gametocytes occur on the day of recurrence they may become a source of misclassification: samples containing gametocytes on the day of recurrence may mistakenly be interpreted as a recrudescence (Snounou & Beck 1998)(Felger & Snounou 2008). Within the samples used in this thesis, none showed appearance of gametocytes under microscopy on the day of recurrence. It cannot be excluded, though, that patients had microscopically undetected gametocytaemia on their day of recurrence.

Asynchronity and sequestration

A single inoculation of an *Anopheles* mosquito may cause multiple infections. *P. falciparum* parasites take seven to 25 days to develop into their clinically apparent stages showing peripheral parasitaemia (Snounou & Beck 1998). Hence, one inoculation may cause parasitaemia in different time points due to a co-infection of parasites.

The peripheral detectability of *P. falciparum* follows a 48-hour periodicity as a consequence of the parasite's life cycle. Late erythrocytic stages sequester into deep tissues and capillaries by cytoadherence to endothelial receptors and are not necessarily detectable in the peripheral blood stream during this time (Falk et al. 2006). Genotyping samples from asymptomatic children over a long-term period has demonstrated that genotypes vary on a daily basis showing different parasites on consecutive days (Farnert et al. 1997). This could also be underlined by Jafari *et al.* (2004) and Missinou *et al.* (2004) who both analysed multiple samples within the first days after administration of the drug. They found that genotypes disappeared and reappeared after a certain time period. This might be explained by varying capillary adhesion characteristics of certain parasites (Jafari et al. 2004).

The two pathomechanisms described above lead to the conclusion that parasites, which have not yet developed into their asexual blood stage or are sequestered, may be overlooked by taking a single blood sample. The consequence is of misclassifying the

sample as a new infection despite it being a co-infection from day 0. A solution to determine a less faulty statement on the true amount of genotypes deriving from the same inoculation could be the examination of multiple samples as suggested by Martensson *et al.* (2007): By taking multiple blood samples within 0 – 3 days after drug administration, 32 additional genotypes could be found in 25 % of patients. Moreover, 18 % of recrudescences were identified only when examining multiple samples. Thus, it may be of interest to enhance a protocol including multiple blood samples after treatment to cover a broader variety of genotypes during the baseline infection on day 0 and therefore being more certain that recurrences are not misclassified. On the other hand, World Health Organization (2008) advises against taking multiple blood samples on consecutive days as it adds costs, possible errors and requires extensive statistical evaluation.

Transmission dynamics

Even though using ITNs is highly recommended in malaria endemic areas, a survey showed that only 66 % of the interviewed people in Burkina Faso had slept underneath an ITN in the previous night (World Health Organization 2016).

The patients investigated in the present study were treated at the local dispensary and then discharged. As *Anopheles* mosquitoes live for up to 30 days (CDC 2017f), the *Anopheles* mosquito that infected a patient the first time might easily re-infect the patient after the drug's activity has diminished. Moreover, the *Anopheles* mosquito might have infected other members of the same family. Hence, different *Anopheles* mosquitoes in the same household can acquire a similar mixture of genotypes because they feed on the same people within one house. They can thus transmit the same population of parasites (Snounou & Beck 1998). Moreover, if the investigated population lives in a small area, this population shares a similar gene pool of malaria parasites. The leading clinical physician of the study site in Bobo-Dioulasso estimated that patients who were enrolled in the study lived zero to four kilometers away from the study site. The proximity of the investigated patients could explain why certain genotypes occurred in high frequencies.

A paired sample showing the same genotype is defined as a recrudescence. In addition to the previously explained mechanisms, a misclassification as a recrudescence could

also occur due to high allele frequencies of certain genotypes: by chance, a person can be infected twice with the same genotype. However, this re-infection with coincidentally the same genotype cannot be differentiated from a recrudescence by CE genotyping. Mathematical parameters P and H_E may help to estimate the possibility of this happening. To gauge the theoretical probability of being infected twice by different parasites with the same genotype, P can be calculated as explained previously. The heterozygosity of infection (H_E) can be calculated to estimate the probability within one population that two samples contain the same genotype.

CE genotyping is an excellent method to investigate PCR-corrected treatment failure rates. However, several above mentioned reasons might lead to misclassifications of infections. It may therefore be indicated to employ more complex statistical models, which estimate more accurately how likely misclassifications are (Falk et al. 2006) (World Health Organization 2008).

4.3 Results of the present study in a broader context

I compared the dataset investigated in this study with similar data from the CATMAP-trial that was conducted in Kilifi, Kenya. The data, which was gained through high-resolution msp-2 CE genotyping comprised fragment sizes and allele-types from paired samples of patients, who had suffered a recurrence of uncomplicated *P. falciparum* malaria. I named the datasets Kilifi-1 and Kilifi-2. I binned the genotypes into 3 bp bins and calculated allele frequencies and recrudescence rates. Moreover, I discussed the results from the present study by comparing them with published genotyping data.

3D7 shows higher polymorphism than D10

Most genotypes being represented > 5 % belonged to the D10-family. However, the polymorphism of genotypes is bigger within the 3D7-family, which leads to a balanced representation of each approximately 50 % of D10-type alleles and 3D7-type alleles. Table 22 and Figures 35 – 36 in the appendix demonstrate the number of different genotypes in Bobo-Dioulasso and in Kilifi as well as the distribution of infections between 3D7-type alleles and D10-type alleles. It can be seen that Bobo-Dioulasso showed the smallest number of different genotypes with 44 genotypes (30 3D7 and 14

D10), whereas Kilifi-1 showed 172 different genotypes (97 3D7 and 75 D10) and Kilifi-2 showed 74 different genotypes (42 3D7 and 32 D10).

A broad variety of genotypes was documented in several published papers; Mwingira *et al.* (2011) found a variety of 116 (83 3D7 and 33 FC27) different msp-2 genotypes at five study sites, of which the study site in Burkina Faso demonstrated 71 genotypes for 3D7 and 26 genotypes for D10. Falk *et al.* (2006) found a variety of 164 different msp-2 genotypes in Ghana (116 3D7 and 48 FC27) and Schoepflin *et al.* (2009) who compared a high transmission area in Tanzania with a low transmission area in Papua New Guinea found 76 and 35 different msp-2 genotypes, respectively (59 3D7 and 17 D10 in Tanzania, 27 3D7 and 8 D10 in Papua New Guinea).

Interestingly, 3D7 showed consistently a broader polymorphism than D10 in all of the analysed datasets and in the published data. A second interesting fact is that the investigated samples from Bobo-Dioulasso showed lower polymorphism that the compared data. A reason to explain this could be the small sample size of n = 37. Kilifi-1 and the published studies analysed bigger sample sizes above 100 samples. On the other hand, Kilifi-2 showed nearly twice as many genotypes than Bobo-Dioulasso with a similar sample size of n = 47. Thus, the sample size cannot be the only factor determining the polymorphism of msp-2. Other factors such as transmission intensity have to be taken into consideration.

Identical genotypes are overrepresented

Certain genotypes occur in high frequencies in Bobo-Dioulasso, in Kilifi and also in published data examining samples from Burkina Faso. Table 22 in the appendix demonstrates a comparison between the genotypes in Bobo-Dioulasso and in Kilifi, which are overrepresented with an allele frequency > 3 %. Before exclusion of this genotype, D10 336 bp was the genotype with the highest frequency of 16.42 % in Bobo-Dioulasso. It was as high as 5.33 % in the Kilifi-1 and of 4.36 % in the Kilifi-2 cohort. Results from Mwingira *et al.* (2011), who examined samples from Burkina Faso using CE genotyping, confirmed these findings. Mwingira and coworkers published that within their examined population the genotype D10 336 bp held the highest allele frequency with 9 % in Burkina Faso. The exclusion of D10 336 bp was necessary in this

thesis due to possible bias. It can be shown, though, that it is known to be a genotype, which appears in a high frequency in Burkina Faso and in Kilifi.

After exclusion of D10 336 bp, the two genotypes with the highest allele frequencies were D10 417 bp with 13.08 % and D10 371 bp with 11.22 %. In the Kilifi-1 dataset, D10 371 bp was the most prominent genotype with a frequency of 6.53 %. The study of Mwingira *et al.* (2011) underlines these findings as they found, that these genotypes were represented within the three most frequent genotypes with an allele frequency of 4 % for D10 417 bp and D10 371 bp, respectively.

Published data from different locations found similarly high allele frequencies within their examined populations: Falk *et al.* (2006) published that the genotype with the highest allele frequency was of 14 % and Schoepflin *et al.* (2009) of 11.2 %.

Remarkably, the analyses did show that first, each population contains prominent genotypes and that second, these prominent genotypes belong to the D10-family. To understand if identical genotypes occurred in high allele frequencies in Bobo-Dioulasso as well as in the Kilifi datasets I constructed Table 22 that can be seen in the appendix. The table illustrates that despite the immense distance between the study sites at which the samples were collected, most prominent genotypes in Bobo-Dioulasso could also be detected among the most frequent genotypes in the Kilifi-datasets. This may suggest that certain genotypes stand under less selection pressure and therefore thrive over big parts of the African continent.

D10-type alleles cause most recrudescences

The results of the Kilifi-datasets demonstrated that most recrudescences were caused by D10-type alleles. In Bobo-Dioulasso, D10-type alleles were responsible for 50 % of recrudescences. The Kilifi-1 dataset revealed that 75.67 % of recrudescences occurred due to D10-type alleles, of which six genotypes showed a recrudescence rate of > 5 % and were responsible for 62.17 % of all recrudescences. Figures 37 – 38 in the appendix show the allele frequencies within recrudescences in Kilifi-1 and Kilifi-2. The Kilifi-2 data showed that 83.31 % of recrudescences occurred due to D10-type alleles.

In spite of the geographical distance between Bobo-Dioulasso and Kilifi, analyses between these cohorts showed that D10-type alleles were clearly overrepresented in both Kilifi cohorts and the Bobo-Dioulasso cohort. Moreover, D10-type alleles were

likely to be responsible for more than one recrudescence each. This leads to the question whether certain D10-type genotypes are more dominant than others and whether they somehow are more likely to provoke recrudescences than 3D7-type alleles.

Looking at the three datasets, it stands out that there are always overrepresented genotypes responsible for recrudescences. In Bobo-Dioulasso, it is D10 371 bp and D10 417 bp, which are responsible for 50 % of recrudescences. In Kilifi-1 it is D10 371 bp that is responsible for 18.92 % of recrudescences and in Kilif-2 it is D10 264 bp that is responsible for 25 % of recrudescences. All most prominent recrudescences are caused by a D10-type allele. To track down whether the genotypes found in recrudescences are in proportion to their population I constructed Tables 23 – 24 for Kilifi-1 and Kilifi-2, which can be seen in the appendix. It stands out that genotypes responsible for recrudescences were not always in proportion with their frequency in the baseline population.

Falk *et al.* (2006) analysed the duration of infections and showed that turnover rates for 3D7 were higher than for FC27 (D10) genotypes and stated that this may indicate that FC27 genotypes are more robust against being eliminated through the host's immune system. Even though the duration of infections was not explicitly determined, the results in the study at hand confirm such a hypothesis as most genotypes that were represented in a high frequency belonged to the D10-family and were not necessarily in proportion with their appearance at baseline. The higher frequency of D10 genotypes in recrudescences might suggest that infections with D10-type alleles bring a higher risk of recrudescence. Further analyses on a bigger sample size should be awaited to confirm this hypothesis.

Recrudescence rates

The recrudescence rates of the study at hand with 21.62 % recrudescences in total and of 25 % in samples of the AL- and the PA-treatment arm are alarmingly high. World Health Organization (2008) recommends retesting when the PCR-corrected treatment failure rate exceeds 10 % or the MOI passes four. However, the study at hand was conducted with a small sample size that does not allow conclusions concerning the treatment failure rates or the efficacy. The transferability of the results is especially limited for samples from patients who were treated with DP or PA as the samples sizes

consisted of four paired samples, respectively. To gain statistically relevant results I highly recommend examining a larger sample size of patients that were enrolled in the WANECAM-trial in Bobo-Dioulasso. This will lead to a more valuable statement about PCR-corrected treatment failure rates of AL, DP and PA in Bobo-Dioulasso. Also, results from other study sites of the WANECAM-trial both concerning recrudescence rates and allele frequencies should be compared to gain further information about allele frequencies in different settings in Western Africa.

Ultimately, when allele frequencies for certain genotypes are high, samples can incorrectly be classified as recrudescences even though the cause for the recurrence is a new infection with a parasite holding the same msp-2 genotype as the parasite infecting the patient the first time. Reasons for this misclassification are explained in preceding chapters. Putting alleles, which appeared in a high frequency in the power of two is a possibility of calculating the risk of falsely classifying new infections as recrudescences. It could be shown that this possibility of incorrectly misclassifying recrudescences is negligibly low for the examined population.

MOI, P and H_E

The MOI is dependent from the transmission intensity. High transmission areas are likely to show a higher MOI than low transmission areas. The results form this study with a MOI = 2.89 correspond to the observation that MOI increases in high transmission areas compared to low transmission areas (Schoepflin et al. 2009). Comparable data from Mwingira *et al.* (2011) found a MOI of 3.03 in Burkina Faso and Schoepflin *et al.* (2009) showed and MOI of 3.72 in Tanzania, which underline the findings from this study. The MOI in a low transmission area on the other hand is reflected exemplary by an MOI of 1.84 in Papua New Guinea (Schoepflin et al. 2009).

Another important factor is the theoretical probability P of being infected twice with an identical genotype. The probability of two infections randomly being caused by the same genotype decreases when the polymorphisms for the investigated marker gene is high (Snounou & Beck 1998). Values of $P < 0.05$ indicate a low probability of being re-infected with the same genotype by two different parasites (Gatton & Cheng 2008). Therefore, the result from the study at hand with $P = 0.0486$ reflects that it is not likely to be infected twice by a parasite with the same genotype. The heterozygosity of

infection was calculated to understand the risk of two randomly picked samples carrying a parasite with the same genotype. The result of $H_E = 0.978$ indicates it to be very likely to chose two different genotypes when randomly choosing from the population and therefore stands for a high expected heterozygosity within the examined population. Comparable data by Schoepflin *et al.* (2009) found $H_E = 0.965$ in a trial which was conducted in Tanzania and $H_E = 0.933$ in a trial conducted in Papua New Guinea. Especially the H_E found in Tanzania is comparable to with the H_E found in the study at hand, indicating a similar broad diversity of genotypes in these populations.

This data suggests that for the examined population, analysing only msp-2 is sufficient as it shows a high discriminatory power. It has to be repeated, though, that due to the small sample size there may be a bias and therefore studies with greater sample size have to be undertaken to assure that examining only msp-2 is sufficient for valid results in the examined area.

4.4 Conclusion and Outlook

The present study demonstrates that CE genotyping was well established at the AG Borrmann laboratory at Eberhard Karls Universität Tübingen. Moreover, it was illustrated that it is an excellent method to determine recrudescence rates and allele frequencies of *P. falciparum* infections.

The results from the present study demonstrate high recrudescence rates for two of the three tested treatments with a recrudescence rate of 25 % for both AL and PA. Looking at these results, it appears that these treatments should be further investigated as World Health Organization (2008) recommends retesting when the recrudescence rates exceed 10 %. However, the study at hand was conducted with a small sample size of four for DP and PA and of 29 for AL. The transferability of the results is therefore limited and does not allow conclusions concerning the treatment failure rates nor the efficacy, as the results are not statistically valid. To be able to make a statement about the efficacy of AL, DP and PA in Bobo-Dioulasso, further analyses on a larger sample size have to be awaited. Also, results from the other study sites of the WANECAM-trial concerning both allele frequencies and recrudescence rates should be compared to obtain valuable information for all three countries.

Even though CE genotyping brings up the previously discussed problems, it still represents the favoured method for *P. falciparum* genotyping. Overall, high resolution CE genotyping remains an excellent tool to determine the characterization of the allele-type and exact fragment length. It shows an advantage towards gel electrophoresis thanks to the improved sensitivity and specificity (Liljander et al. 2009) and has been recommended by World Health Organization (2008) instead of formerly performed gel electrophoresis as it shows a higher discriminatory power especially in high transmission areas. In addition, it provides exact information about parasite populations, multiplicity of infection and frequency distributions in different endemic settings. In the present study, the high reproducibility could be confirmed as results from two different PCRs showed identical results. High resolution CE should also be implemented in developing countries, for example by sharing facilities (World Health Organization 2008). This would accelerate the process of genotyping and results could therefore be interpreted faster.

Investigating more on parasite populations and allele frequencies in different endemic settings would lead to a broader understanding of true recrudescences and allele frequencies and therefore give more valuable information about treatment failures and thus efficacy of drugs. A goal could be the establishment of a map of allele frequencies throughout malaria endemic areas. By observing changes of allele frequencies a further understanding of the dynamics of different allelic families could be obtained. This could lead to a better understanding of transmission of genotypes. Moreover, a possible dominancy of allelic families or certain genotypes could be observed concerning both allele frequencies and recrudescences.

5 Summary

In the context of my dissertation I worked for nine months in Bobo-Dioulasso, Burkina Faso, as part of the WANECAM-trial, which compared the antimalarial agents dihydroartemisinin-piperaquine and pyronaridine-artesunate with the comparator drug artemether-lumefantrine.

The aim of this pilot study was to implement *P. falciparum* merozoite surface protein 2 genotyping using high-resolution capillary electrophoresis genotyping with an automated sequencer at the AG Borrmann laboratory at the Institute of Tropical Medicine of Eberhard Karls Universität Tübingen. I analysed if recurrences were caused by new infections or recrudescences. Furthermore, I determined allele frequencies and recrudescence rates of the studied population.

In paired filter paper blood samples from patients from Bobo-Dioulasso, I extracted *Plasmodium falciparum* DNA, amplified it with a primary polymerase chain reaction and subsequently with a secondary polymerase chain reaction. I analysed the amplification products first by gel electrophoresis and second, using capillary electrophoresis with an automated sequencer. The software GeneScan® evaluated the results and presented them as electropherograms, which I interpreted and analysed.

Of the 63 paired samples, I was able to extract and analyse 37 successfully. I noticed that 3D7-type alleles appeared in higher polymorphisms than D10-type alleles, but that D10-type alleles were responsible for high allele frequencies. I calculated a recrudescence rate of 21.62 % in total. Genotypes from the D10 family, which were highly represented in the baseline population, were also highly represented in recrudescences. For the 3D7 family, a similar proportionality could not be found. The recrudescence rates for artemether-lumefantrine and pyronaridine-artesunate were high with 25 % each. Further analyses with a bigger sample size as well as equal distribution between treatment arms should be awaitened before drawing further conclusions.

The discussion of this study is subdivided into three parts: technical limitations of the methodology, biological aspects of *P. falciparum* and the comparison of my results with published and unpublished data. The technical limitations concerned mostly the

detection limit of *P. falciparum* when examined by CE genotyping. The biological aspects of the parasite's life cycle, which cause difficulties with CE genotyping are firstly, that infections might be misclassified as recrudescences due to occurrence of gametocytes on the day of recurrence and secondly, that *P. falciparum* sequesters into deep tissues and is therefore not always detectable in the blood stream. This can result in certain genotypes not being detected on day 0 even though they have already spread in the human body. A misclassification as a recrudescence may also occur when, by coincidence, patients are re-infected by parasites with the same genotype. Furthermore, I compared my data with published and unpublished data and understood that the results were often consistent with each other: My results as well as the compared results show that firstly, 3D7-type alleles have a higher polymorphism than D10-type alleles, and that secondly each population has certain genotypes that are overrepresented and which tend to belong to D10 genotypes.

The results of this study have shown that CE genotyping was well established for samples from Burkina Faso. The high recrudescence rates in this study are not statistically valid due to small sample size and due to unequal number per treatment arm. Further analyses of the WANECAM-trial should be awaited to draw conclusions concerning the efficacy of the examined drugs. The potential dominance of possible of certain genotypes in parasite populations should be monitored in malaria trials to prevent misinterpretation of genotyping results.

6 Zusammenfassung

Für meine Dissertation arbeitete ich neun Monate lang im Rahmen der WANECAM-Studie, in welcher Dihydroartemisinin-Piperaquin und Pyronaridin-Artesunat mit dem Kontrollmedikament Artemether-Lumefantrin verglichen wurden, in Bobo-Dioulasso in Burkina Faso.

Die Fragestellung meiner Promotionsarbeit betraf die Einrichtung der Genotypisierung des Merozoiten Oberflächenproteins 2 von *Plasmodium falciparum* mit Hilfe der high-resolution Kapillarelektrophorese, welche mit einem automatisierten Sequenziergerät im Labor der AG Borrmann des Instituts für Tropenmedizin, Reisemedizin, Humanparasitologie der Eberhard Karls Universität Tübingen durchgeführt wurde. Ich untersuchte Probenpaare auf Häufigkeiten der Allele in der Population sowie darauf, ob eine Wiedererkrankung auf eine erneute Infektion oder auf eine Rekrudeszenz zurückzuführen war.

Ich extrahierte im Tübinger Labor die *Plasmodium falciparum* DNA aus Filterpapierproben aus Bobo-Dioulasso, amplifizierte diese mit Hilfe einer primären und einer sekundären Polymerase-Kettenreaktion und untersuchte das Amplifikationsprodukt vorerst mittels Agarose-Gelelektrophorese und bei erfolgreicher Extraktion im zweiten Schritt anhand der Kapillarelektrophorese im automatisierten Sequenziergerät.

Von den 63 gepaarten Filterpapierproben konnte ich 37 Paare erfolgreich auswerten. Auffällig war zum einen der höhere Polymorphismus von 3D7 gegenüber D10. Zum anderen zeigte sich, dass einige Genotypen der D10-Familie in einer kleineren Varianz, jedoch jeweils in einer hohen Allelfrequenz auftraten. Es zeigte sich eine Rekrudeszenz-Rate von insgesamt 21.62 %, wobei die Genotypen der D10-Familie, welche am häufigsten in der Population auftraten, auch am häufigsten bei den Rekrudeszenzen vertreten waren. Für Allele der 3D7-Familie zeigte sich diese Proportionalität nicht. Die Rekrudeszenzraten für Artemether-Lumefantrin und Pyronaridin-Artesunat waren besonders hoch mit jeweils 25 %, jedoch sollten weitere Analysen mit einer höheren

Probenanzahl sowie gleichmäßiger Verteilung der Proben zwischen den drei Studienarmen abgewartet werden.

In der Diskussion dieser Arbeit ging ich auf die technischen Einschränkungen der Methodik, die biologischen Aspekte von *Plasmodium falciparum* sowie den Vergleich meiner Ergebnisse mit veröffentlichten und unveröffentlichten Daten ein. Die technischen Einschränkungen betrafen vor allem den Aspekt, dass Plasmodien unter einer gewissen Nachweisgrenze nicht detektiert werden können. Die biologischen Eigenschaften von *Plasmodium falciparum*, welche die Genotypisierung erschweren, betreffen zum einen die falsche Klassifizierung eines Probenpaares als Rekrudeszenz, wenn am Tag der Wiedererkrankung Gametozyten im Blut vorhanden sind. Zum anderen sequestriert *P. falciparum* in Gewebe und ist somit nicht immer im Blut nachweisbar. Dies kann dazu führen, dass einzelne Genotypen am Tag 0 zwar bereits im Körper des Patienten vorhanden, jedoch durch die Sequestrierung nicht nachweisbar sind. Ein weiterer Aspekt ist die falsche Klassifizierung eines Probenpaares als Rekrudeszenz, wenn durch Zufall die Wiedererkrankung durch den gleichen Genotyp von *P. falciparum* hervorgerufen wird. Zum Schluss habe ich meine Ergebnisse mit publizierten und bereitgestellten Daten verglichen. Es hat sich dabei herausgestellt, dass diese in vielerlei Hinsicht miteinander konsistent waren: sowohl meine Ergebnisse als auch die Vergleiche zeigten, dass 3D7 einen höheren Polymorphismus aufzeigt und dass in jeder Population gewisse Genotypen überrepräsentiert sind, die besonders häufig der D10-Familie angehören.

Die Ergebnisse dieser Studie zeigen, dass die Genotypisierung für Proben von Parasitenisolaten aus Burkina Faso erfolgreich eingerichtet werden konnte. Die hohen Rekrudeszenzraten, die in dieser Studie gefunden wurden, sind auf Grund der geringen Fallzahl nicht statistisch aussagekräftig. Um eine Aussage über die Effizienz der Medikamente zu treffen, sollten die Gesamtergebnisse der WANECAM-Studie abgewartet werden. Die potenzielle Dominanz von bestimmten, lokal vermehrt vorkommenden Parasiten-Genotypen sollte weiterhin kontinuierlich überprüft werden, um eine Fehlinterpretation von Malariastudien durch systematische Fehler bei der Genotypisierung zu verhindern.

7 Bibliography

Achan, J. et al., 2011. Quinine, an old anti-malarial drug in a modern world: role in the treatment of malaria. *Malaria journal*, 10(1), p.144. Available at: http://www.malariajournal.com/content/10/1/144.

Arama, C. & Troye-Blomberg, M., 2014. The path of malaria vaccine development: Challenges and perspectives. *Journal of Internal Medicine*, 275(5), pp.456–466.

Ashley, E. a et al., 2014. Spread of Artemisinin Resistance in Plasmodium falciparum Malaria. *New England Journal of Medicine*, 371(5), pp.411–423. Available at: http://www.nejm.org/doi/abs/10.1056/NEJMoa1314981 [Accessed July 31, 2014].

Ashley, E. a & White, N.J., 2014. The duration of Plasmodium falciparum infections. *Malaria journal*, 13(1), p.500.

Basco, L.K., Tahar, R. & Escalante, A., 2004. Molecular epidemiology of malaria in Cameroon. XVIII. Polymorphisms of the Plasmodium falciparum merozoite surface antigen-2 gene in isolates from symptomatic patients. *American Journal of Tropical Medicine and Hygiene*, 70(3), pp.238–244.

Bassat, Q. et al., 2009. Dihydroartemisinin-piperaquine and artemether-lumefantrine for treating uncomplicated malaria in African children: a randomised, non-inferiority trial. *PloS one*, 4(11), p.e7871. Available at: http://www.pubmedcentral.nih.gov/articlerender.fcgi?artid=2776302&tool=pmcentrez&rendertype=abstract [Accessed October 28, 2014].

Borrmann, S. et al., 2011. Declining responsiveness of Plasmodium falciparum infections to artemisinin-based combination treatments on the Kenyan coast. *PloS one*, 6(11), p.e26005. Available at: http://www.pubmedcentral.nih.gov/articlerender.fcgi?artid=3213089&tool=pmcentrez&rendertype=abstract [Accessed October 21, 2014].

Bousema, T. & Drakeley, C., 2011. Epidemiology and Infectivity of Plasmodium falciparum and Plasmodium vivax Gametocytes in Relation to Malaria Control and Elimination. *Clinical Microbiology Reviews*, 24(2), pp.377–410.

Boyle, M.J. et al., 2014. Sequential processing of Merozoite Surface Proteins during

and after Erythrocyte Invasion by Plasmodium falciparum. *Infection and Immunity*, 82(3), pp.924–936.

Campo, B. et al., 2015. Killing the hypnozoite - drug discovery approaches to prevent relapse in Plasmodium vivax. *Pathogens and global health*, 109(3), pp.107–22. Available at: http://www.maneyonline.com/doi/abs/10.1179/2047773215Y.0000000013.

Collins, W.J. et al., 2006. The use of genotyping in antimalarial clinical trials: a systematic review of published studies from 1995-2005. *Malaria journal*, 5, p.122.

Cox, F.E., 2010. History of the discovery of the malaria parasites and their vectors. *Parasites & Vectors*, 3(1), p.5.

Dondorp, A.M. et al., 2010. Artemisinin resistance: current status and scenarios for containment. *Nature Publishing Group*, 8(4), pp.272–280. Available at: http://dx.doi.org/10.1038/nrmicro2331.

Ezzet, F. et al., 2000. Pharmacokinetcis and pharmacodynamics of lumefanthrine (benflumetol) in acute falciparum malaria. *Antimicrobial Agents and Chemotherapy*, 44(3), pp.697–704. Available at: http://dx.doi.org/10.1128/AAC.44.3.697-704.2000.

Falk, N., Maire, N., Sama, W., Owusu-Agyei, S., et al., 2006. Comparison of PCR-RFLP and genescan-based genotyping for analyzing infection dynamics of Plasmodium falciparum. *American Journal of Tropical Medicine and Hygiene*, 74(6), pp.944–950.

Farnert, A. et al., 1997. Daily dynamics of Plasmodium falciparum subpopulations in asymptomatic children in a holoendemic area. *American Journal of Tropical Medicine and Hygiene*, 56(5), pp.538–547.

Felger, I. & Snounou, G., 2008. Recommended Genotyping Procedures (RGPs) to identify parasite populations, pp.1–44.

Gatton & Cheng, Q., 2008. Can estimates of antimalarial efficacy from field studies be improved? , 24(2), pp.68–73.

Guttmann, P. & Ehrlich, P., 1891. Ueber die Wirkung von Methylenblau bei Malaria. *Berliner Klinische Wochenschrift*, 39, pp.953–956. Available at: http://www.thieme-connect.de/DOI/DOI?10.1055/s-0028-1138168.

Jafari, S. et al., 2004. Plasmodium falciparum clonal population dynamics during

malaria treatment. *The Journal of infectious diseases*, 189, pp.195–203.

Joshi, H. et al., 2007. Genetic structure of Plasmodium falciparum field isolates in eastern and north-eastern India. *Malaria Journal*, 1(6), pp.2–9.

Kiwanuka, G.N., 2009. Genetic diversity in Plasmodium falciparum merozoite surface protein 1 and 2 coding genes and its implications in malaria epidemiology: a review of published studies from 1997-2007. *Journal of vector borne diseases*, 46(1), pp.1–12. Available at: http://www.ncbi.nlm.nih.gov/pubmed/19326702 [Accessed April 22, 2016].

Klayman, D.L., 1985. Qinghaosu (Artemisinin): An Antimalarial Drug from China. *Science*, 228, pp.1049–1055.

ter Kuile, F. et al., 1993. Plasmodium falciparum: in vitro studies of the pharmacodynamic properties of drugs used for the treatment of severe malaria. *Experimental parasitology*, 76(1), pp.85–95. Available at: http://www.ncbi.nlm.nih.gov/pubmed/8467901.

Liljander, A. et al., 2009. Optimization and validation of multi-coloured capillary electrophoresis for genotyping of Plasmodium falciparum merozoite surface proteins (msp1 and 2). *Malaria Journal*, 8(1), p.78. Available at: http://malariajournal.biomedcentral.com/articles/10.1186/1475-2875-8-78.

MacRaild, C.A. et al., 2015. Conformational dynamics and antigenicity in the disordered malaria antigen merozoite surface protein 2. *PLoS ONE*, 10(3), pp.1–18.

Makanga, M. & Krudsood, S., 2009. The clinical efficacy of artemether / lumefantrine (Coartem ®). *Malaria Journal*, 12, pp.1–12.

Martensson, A. et al., 2007. Influence of consecutive-day blood sampling on polymerase chain reaction-adjusted parasitological cure rates in an antimalarial-drug trial conducted in Tanzania. *The Journal of infectious diseases*, 195(4), pp.597–601. Available at: http://www.ncbi.nlm.nih.gov/pubmed/17230421.

Messerli, C. et al., 2016. Critical evaluation of molecular monitoring in malaria drug efficacy trials: pitfalls of length polymorphic markers. *Antimicrobial Agents and Chemotherapy*, 61(1), p.AAC.01500-16. Available at: http://aac.asm.org/lookup/doi/10.1128/AAC.01500-16.

Millar, S.B. & Cox-Singh, J., 2015. Human infections with Plasmodium knowlesi-

zoonotic malaria. *Clinical microbiology and infection : the official publication of the European Society of Clinical Microbiology and Infectious Diseases*, 21(7), pp.640–8. Available at: http://www.ncbi.nlm.nih.gov/pubmed/25843504 [Accessed April 23, 2016].

Miller, L.H. et al., 2002. The pathogenic basis of malaria, Miller 2002. *Nature*, 415(February), pp.673–679.

Missinou, M. a, Kun, J.F.J. & Kremsner, P.G., 2004. No change in parasite genotype during single episodes of Plasmodium falciparum malaria in Gabonese children. *Parasitology research*, 93(4), pp.322–7. Available at: http://www.ncbi.nlm.nih.gov/pubmed/15185144.

Mordmüller, B. et al., 2017. Sterile protection against human malaria by chemoattenuated PfSPZ vaccine. *Nature Publishing Group*, 542(7642), pp.445–449. Available at: http://dx.doi.org/10.1038/nature21060.

Mwingira, F. et al., 2011. Plasmodium falciparum msp1, msp2 and glurp allele frequency and diversity in sub-Saharan Africa. *Malaria journal*, 10(1), p.79. Available at: http://malariajournal.biomedcentral.com/articles/10.1186/1475-2875-10-79.

Noedl, H., Socheat, D. & Satimai, W., 2009. Artemisinin-Resistant Malaria in Asia. *New England Journal of Medicine*, 361;5(July), pp.540–541.

Nosten, F. & White, N.J., 2007. Artemisinin-Based Combination Treatment of Falciparum Malaria. *The American Journal of Tropical Medicine and Hygiene*, 77(Suppl 6), pp.181–192.

Packard, R.M., 2014. The Origins of Antimalarial-Drug resistance. *The New England Journal of Medicine*, 78(3), p.407.

Partnership, C.T., 2015. Efficacy and safety of RTS,S/AS01 malaria vaccine with or without a booster dose in infants and children in Africa : final results of a phase 3, individually randomised, controlled trial. *The Lancet*, 386(9988), pp.31–45. Available at: http://dx.doi.org/10.1016/S0140-6736(15)60721-8.

Partnership, C.T., 2014. Efficacy and Safety of the RTS , S / AS01 Malaria Vaccine during 18 Months after Vaccination : A Phase 3 Randomized , Controlled Trial in Children and Young Infants at 11 African Sites. *Plos one*, 11(7), pp.1-24.

Pfeil, J., Borrmann, S. & Tozan, Y., 2014. Dihydroartemisinin-Piperaquine v.

Artemether-Lumefantrine for First-Line Treatment of Uncomplicated Malaria in African Children : A Cost-Effectiveness Analysis. *PLoS ONE*, 9(4), pp.6–12.

Roper, C. et al., 2004. Intercontinental Spread of Pyrimethamine-Resistant Malaria. *Science*, 305(5687), pp.1124–1124. Available at: http://www.sciencemag.org/cgi/doi/10.1126/science.1098876.

Ross, R., 2002. The role of the mosquito in the evolution of the malarial parasite: the recent researches of Surgeon-Major Ronald Ross, I.M.S. 1898. *Yale Journal of Biology and Medicine*, 75(2), pp.103–105.

Sagara, I. et al., 2016. Safety and effi cacy of re-treatments with pyronaridine-artesunate in African patients with malaria: a substudy of the WANECAM randomised trial. *Lancet*, 16, pp.189–198.

Samadoulougou, S. et al., 2014. Multilevel and geo-statistical modeling of malaria risk in children of Burkina Faso. *Parasites & vectors*, 7(1), p.350. Available at: http://www.parasitesandvectors.com/content/7/1/350.

Schoepflin, S. et al., 2009. Comparison of Plasmodium falciparum allelic frequency distribution in different endemic settings by high-resolution genotyping. *Malaria journal*, 8, p.250. Available at: http://www.pubmedcentral.nih.gov/articlerender.fcgi?artid=2774868&tool=pmcentrez&rendertype=abstract [Accessed October 28, 2014].

Shin Poong Pharmaceutical Co., Summary of Product Characteristics of Pyramax 180 mg/60mg Film-coated Tablets.

Siciliano, G. & Alano, P., 2015. Enlightening the malaria parasite life cycle: Bioluminescent Plasmodium in fundamental and applied research. *Frontiers in Microbiology*, 6(MAY), pp.1–8.

Sigma-Tau Industrie Framaceutiche Riunite s.p.a., 2011. Summary of Product Characteristics of Eurartesim 160 mg/20 mg Film-coated Tablets. , pp.1–55.

Smythe, J.A. et al., 1991. Structural diversity in the Plasmodium falciparum merozoite surface antigen 2. *Immunology*, 88(March), pp.1751–1755.

Snounou, G. & Beck, H.-P., 1998. The Use of PCR Genotyping in the Assessment of Recrudescence or Reinfection after Antimalarial Drug Treatment. *Parasitology Today*, 14(11), pp.462–467.

Tinto, H. et al., 2002. Chloroquine and sulphadoxine-pyrimethamine efficacy for

uncomplicated malaria treatment and haematological recovery in children in Bobo-Dioulasso, Burkina Faso during a 3-year period 1998-2000. *Tropical Medicine and International Health*, 7(11), pp.925–930.

Tinto, H. et al., 2016. Lessons learnt from 20 years surveillance of malaria drug resistance prior to the policy change in Burkina Faso. *Annals of parasitology*, 62(1), pp.17–24. Available at: http://www.ncbi.nlm.nih.gov/pubmed/27262953.

Walsh, P.S., Fildes, N.J. & Reynolds, R., 1996. Sequence analysis and characterization of stutter products at the tetranucleotide repeat locus vWA. *Nucleic Acids Research*, 24(14), pp.2807–2812.

White, N.J. et al., 2015. Malaria. *Lancet*, 22(3), pp.25–32.

White, N.J. & Properties, P., 2008. Qinghaosu (Artemisinin): The Price of Success. *Science*, 320(April), pp.330–335.

WHO, Barrette, A. & Ringwald, P., 2010. Global Report On Antimalarial Drug Efficacy And Drug Resistance: 2000-2010. *World Health Organization*. Available at: http://www.pubmedcentral.nih.gov/articlerender.fcgi?artid=3319253&tool=pmcentrez&rendertype=abstract.

Wickham, M.E., Thompson, J.K. & Cowman, A.F., 2003. Characterisation of the merozoite surface protein-2 promoter using stable and transient transfection in Plasmodium falciparum. *Molecular & Biochemical Parasitology, Elsevier*, 129, pp.147–156.

Witkowski, B. et al., 2013. Novel phenotypic assays for the detection of artemisinin-resistant Plasmodium falciparum malaria in Cambodia: In-vitro and ex-vivo drug-response studies. *The Lancet Infectious Diseases*, 13(12), pp.1043–1049. Available at: http://dx.doi.org/10.1016/S1473-3099(13)70252-4.

Wootton, J.C. et al., 2002. Genetic diversity and chloroquine selective sweeps in Plasmodium falciparum. *Nature*, 418(6895), pp.320–323. Available at: http://www.nature.com/doifinder/10.1038/nature00813.

World Health Organization, 2015. Guidelines for the Treatment of Malaria. *WHO Press*, (Third edition), pp.71–88.

World Health Organization, 2008. Methods and techniques for clinical trials on antimalarial drug efficacy : genotyping to identify parasite populations. An

informal consultation organized by the Medicines for Malaria Venture and cosponsored by the World Health Organization, 29-31 May 200. *WHO Press*, (May), pp.1–16.

World Health Organization, 2016. World Malaria Report 2016, *World Health Organization*.

Internet bibliography

Burkina Faso : chronique d'une crise annoncée. Available at http://www.lemonde.fr/idees/article/2015/09/30/burkina-faso-chronique-d-une-criseannoncee_4777962_3232.html?xtmc=burkina_faso_30_octobre_2014&xtcr=15 [Accessed January 20, 2017a].

Centers for Disease Control and Prevention. Anopheles Mosquitoes. Available at https://www.cdc.gov/malaria/about/biology/mosquitoes/ [Accessed June 05, 2017f]

Etat et Structure de la Population, 2012. Institut National de la Statistique et de la Démographie du Burkina Faso. Available at http://www.insd.bf/pages_web/donnee_stat/structurelle/Fichiers%20PDF/Tableau%201%201.pdf [Accessed January 20, 2017g]

Ex-Premier Marc Christian Kaboré wird Präsident in Burkina Faso. Available at http://www.faz.net/aktuell/politik/ausland/afrika/ex-premier-marc-christian-kabore-wird-praesident-in-burkina-faso-13942027.html [Accessed January 20, 2017d].

INSD, 2013. Annuaire statistique 2012. *Institut National de la Statistique et de la Démographie*. Available at: www.insd.bf/n/contenu/pub_periodiques/annuaires_stAt/Annuaires_stat_nationaux_BF/Annuaire_stat_2012.pdf [Accessed December 25, 2017].

INSD, 2015. Annuaire statistique 2016. *Institut national de la statistique et de la demographie*, p.350. DOI: 10.1007/s13398-014-0173-7.2 Available at www.insd.bf/n/contenu/pub_periodiques/annuaires_stat/Annuaires_stat_nationaux_BF/Annuaire_stat_2015.pdf [Accessed January 19, 2017].

Six jours qui ont changé le Burkina Faso. *LeMonde.* Available at: http://www.lemonde.fr/afrique/article/2014/11/03/six-jours-qui-ont-change-le-

burkina-faso_4517145_3212.html?xtmc=burkina_faso_chute_compaore&xtcr=92 [Accessed January 20, 2017e].

Tote und Verletzte nach Militärputsch in Burkina Faso | ZEIT ONLINE. Available at: http://www.zeit.de/politik/ausland/2015-09/burkina-faso-au-setzt-mitgliedschaft-aus-putsch [Accessed January 20, 2017b].

Übergangsregierung löst Putschisten-Einheit RSP auf | ZEIT ONLINE. Available at: http://www.zeit.de/politik/2015-09/burkina-faso-putschisten-einheit [Accessed January 20, 2017c].

UNdata | country profile | Burkina Faso. Available at: http://data.un.org/CountryProfile.aspx?crName=burkina faso [Accessed June 3, 2016f].

Statement of Originality

I conducted experimental work for this thesis at the "Institut für Tropenmedizin, Reisemedizin, Humanparasitologie der Eberhard Karls Universität" under the supervision of Professor Steffen Borrmann. I conducted the experiments for this thesis after introduction to the laboratory work by the laboratory technician Martina Henk. She conducted the experiments, which are referred to as "Genotyping-2016" in the text. I myself conducted all other experiments.

Professor Borrmann provided me with two datasets in form of Excel tables from the CATMAP clinical trial (clinical trial registry: NCT01190371), which was conducted in Kilifi, Kenya. I performed statistical calculations from these datasets, which are included in this thesis and referred to as "Kilifi-1" and "Kilifi-2".

The clinical, parasitological, biochemical and haematological data, which were collected within the WANECAM clinical trial (Clinical trial registry: PACTR20115000286876) was facilitated by Professor Abdoulaye Djimdé and Professor Jean-Bosco Ouédraogo.

Any ideas or quotations from the work of other people, published or otherwise, are fully acknowledged in accordance with the standard referencing practices of the discipline.

I certify that this thesis and the research to which it refers are the product of my own work.

München, 22.12.2017

Appendix

7.1 Extended study design

Inclusion criteria

To be included in the study, patients had to be above a certain age and weight according to the treatment arm. Patients necessarily had to present with fever above 37.5 °C or history of fever in the last 24 hours and positive microscopy of *Plasmodium sp.* with a density less than 200 000 / µl. Patients had to be able to swallow oral medication and could only be included, if the anamnesis showed no treated malaria episodes in the last two weeks. A written informed consent had to be signed and the patient had to be able and willing to participate for the follow-up visits.

Non inclusion criteria

Patients enrolled in the study could not meet any signs or symptoms of severe malaria requiring parenteral treatment. No severe vomiting, no history or evidence of cardiovascular, respiratory, hepatic, renal, gastrointestinal, immunological, neurological, endocrine, psychiatric disorders, jaundice, infections, malignancy, convulsions or other abnormalities. The hemoglobin level had to be > 7 g / dl, ALT levels and creatinine levels had to be under a certain range. Women with childbearing potential must not be pregnant or planning on becoming pregnant nor lactating. Patients with knowledge of positive HIV antibodies, HAV-IgM, HBsAg or HCV antibodies were not included in the study. Patients known or suspected to abuse alcohol were not included as little as patients who had had treatment with any antimalarial agent in the past two weeks prior to inclusion or any investigational drug within 4 weeks prior to inclusion.

Diagnostics of P. *falciparum* malaria

To diagnose a malaria infection, two separate *Giemsa* stained thick and thin films were examined. The slides were examined with a binocular microscope and an oil immersion

lens. Thick films were analysed to whether the sample contained *Plasmodium sp*. or not. If no *Plasmodium sp.* was observed in 100 fields the slide was declared negative.

If the thick film was positive for *Plasmodium sp.*, asexual forms were counted against leukocytes based on the formula shown below:

$$Parasite\ density\ per\ \mu l\ = \frac{number\ of\ Plasmodium\ parasites \times actual\ leukocytes}{number\ of\ leukocytes\ counted\ (200)}$$

If the parasite count was below 10, the count was increased to 500 leukocytes and if gametocytes were seen, a gametocyte count was performed against 1000 leukocytes.

Drug administration

If an uncomplicated malaria infection was confirmed microscopically, the randomly attributed study drug was administered at the health center under supervision of a study team member. Therefore, AL was applied orally twice a day and DP and PA were given orally once a day for three consecutive days on day 0, day 1 and day 2 after inclusion.

Artemether-lumefantrine

AL was administered twice daily for three days. Water and food was given at the same time, as AL is absorbed better in the presence of fats. The dosage of the tablet was of 20:120 mg. AL was given as Coartem® by Novartis Pharmaceutical Company.

Table 19: Dosage artemether lumefantrine

Body weight	**No. of tablets**
5 to < 15 kg	1 (dispersible)
15 to < 25 kg	2 (dispersible)
25 to < 35 kg	3
≥ 35 kg	4

Dihydroartemisinin-piperaquine

DP was given once daily for three days. It was taken with water and without food. The tablets were given no less than 3 hours after the last meal and patients remained without food for 3 hours after drug administration.

DP was given as Eurartesim® by Sigma-Tau Pharma.

Table 20: Dosage dihydroartemisinin-piperaquine

Body weight	Dose of tablet	Amount of tablets
5 to < 7 kg	20:160 mg	½
7 to < 13 kg	20:160 mg	1
13 to < 24 kg	40:320 mg	1
24 to < 36 kg	40:320 mg	2
36 to < 75 kg	40:320 mg	3
75 to 100 kg	40:320 mg	4

Pyronaridine-artesunate

PA was administered once a day for three days depending on the patient's body weight: from 5 – 20 kg body weight in sachets with a dosage of (pyronaridine:artesunate) of (60:20 mg), and above 20 kg body weight in tablets with a dosage of (P:A) of (180:60mg). Phase II and Phase III studies on healthy patients and patients with malaria had show efficiency and safety at a dose-level range of 7.5:2.5 mg / kg to 15:5 mg / kg PA. To secure the safety of PA, a Data Safety and Monitoring Board (DSMB) evaluated data from the first 20 and 40 patients after the second treatment course with PA.
PA was given as Pyramax® by Shin Poong Pharmaceutical.

Table 21: Dosage pyronaridine-artesunate

Body weight	No. of sachets	Body weight	No. of tablets
5 to < 8 kg	1	20 to < 24 kg	1
8 to < 15 kg	2	24 to < 45 kg	2
15 to < 20 kg	3	45 to < 65 kg	3
		65 to < 90 kg	4

Ethical approval

The Investigator Brochure, the Product Monographs, the signed protocol and the Final Informed Consent Form were submitted to the local Ethics Committee (EC). The final version of the informed consent form was approved by the local EC. Final approval by

the EC and the relevant national Regulatory Authority were provided to the Sponsor before the first patient was enrolled in the study.

The investigators or sponsors submitted progress reports to the EC according to local regulations and guidelines. The study was conducted in compliance with the study protocol. The informed consent was obtained according to the ethical principles stated in the Declaration of Helsinki 2000 version, the applicable guidelines for ICH GCP and the applicable local laws and regulations.

The information about the WANECAM-trial is not complete. The fundamental information for the present study was given, but further details were not amplified in the thesis at hand.

7.2 Tables

Table 22: Number of different genotypes in Bobo-Dioulasso, Kilifi-1 and Kilifi-2

Allelic type	Genotypes Bobo-Dioulasso	Genotypes Kilifi-1	Genotypes Kilifi-2
3D7 & D10	44	172	74
3D7	30	97	42
D10	14	75	32

Table 23: Comparing allele frequencies of genotypes in Bobo-Dioulasso, Kilifi-1 and Kilifi-2 of genotypes that occurred > 3 %

Bobo-Dioulasso	Kilifi-1	Kilifi-2
D10 336 bp excluded	D10 371 bp 6.53 %	3D7 272 bp 6.04 %
D10 417 bp 13.08 %	D10 336 bp 5.33 %	D10 264 bp 5.03 %
D10 371 bp 11.22 %	D10 261 bp 4.13 %	D10 336 bp 4.36 %
3D7 272 bp 5.61 %	D10 298 bp 3.59 %	D10 371 bp 4.36 %
3D7 281 bp 4.67 %		D10 298 bp 3.69 %
3D7 242 bp 3.74 %		D10 354 bp 3.69 %
3D7 254 bp excluded		D10 407 bp 3.69 %
3D7 264 bp 3.74 %		
3D7 276 bp 3.74 %		

D10 407 bp 3.74 %

Table 24: Genotypes responsible for recrudescences in Kilifi-1: comparing the allele frequencies of these genotypes in the baseline population and in recrudescences

Genotype (bp)	**Allele frequency Kilifi-1 population (%)**	**Allele frequency Kilifi-1 recrudescences (%)**
D10: 371	6.53	18.92
D10: 336	5.33	13.51
D10: 261	4.13	10.81
D10: 298	3.59	8.11
D10: 455	2.72	5.41
D10: 264	1.85	5.41
3D7: 251	0.87	2.70
3D7: 272	1.74	2.70
3D7: 281	1.31	2.70
3D7: 297	1.09	2.70
3D7: 300	0.65	2.70
3D7: 318	0.87	2.70
3D7: 340	1.63	2.70
3D7: 372	0.76	2.70
3D7: 393	0.87	2.70
D10: 345	1.41	2.70
D10: 360	1.85	2.70
D10: 363	0.33	2.70
D10: 386	0.65	2.70
D10: 407	1.09	2.70

Table 25: Genotypes responsible for recrudescences in Kilifi-2: comparing the allele frequencies of these genotypes in the baseline population and in recrudescences

Genotype (bp)	Allele frequency Kilifi-2 population (%)	Allele frequency Kilfi-2 recrudescences (%)
D10: 264	5.03	25.00
D10: 316	1.01	8.33
D10: 354	3.69	8.33
D10: 359	2.01	8.33
D10: 371	4.36	8.33
D10: 389	2.01	8.33
D10: 424	1.01	8.33
D10: 455	2.68	8.33
3D7: 276	1.68	8.33
3D7: 281	2.68	8.33

7.3 Figures

In the following electropherogram and pie charts, 3D7-type alleles are represented in green colour, whereas D10-type alleles are depicted in blue colour.

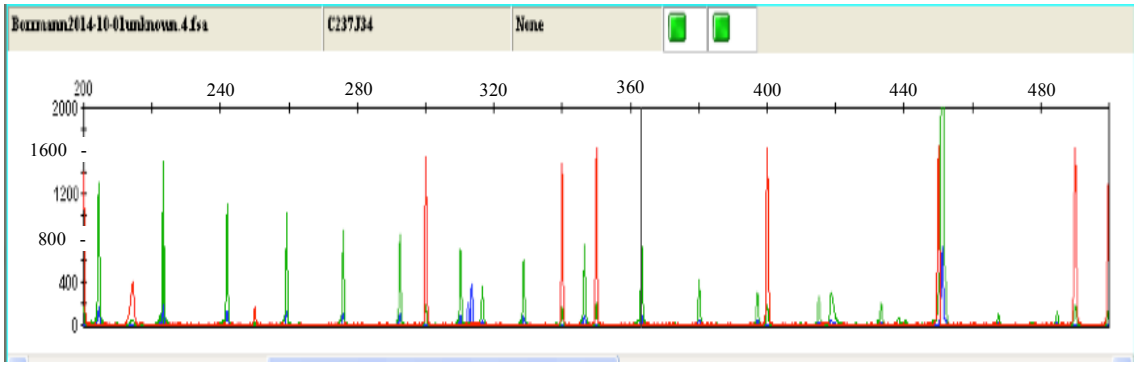

Figure 34: Stutter peaks. X-axis shows length of detected PCR-fragments in bp. Y-axis depicts detected intensity in rfu.

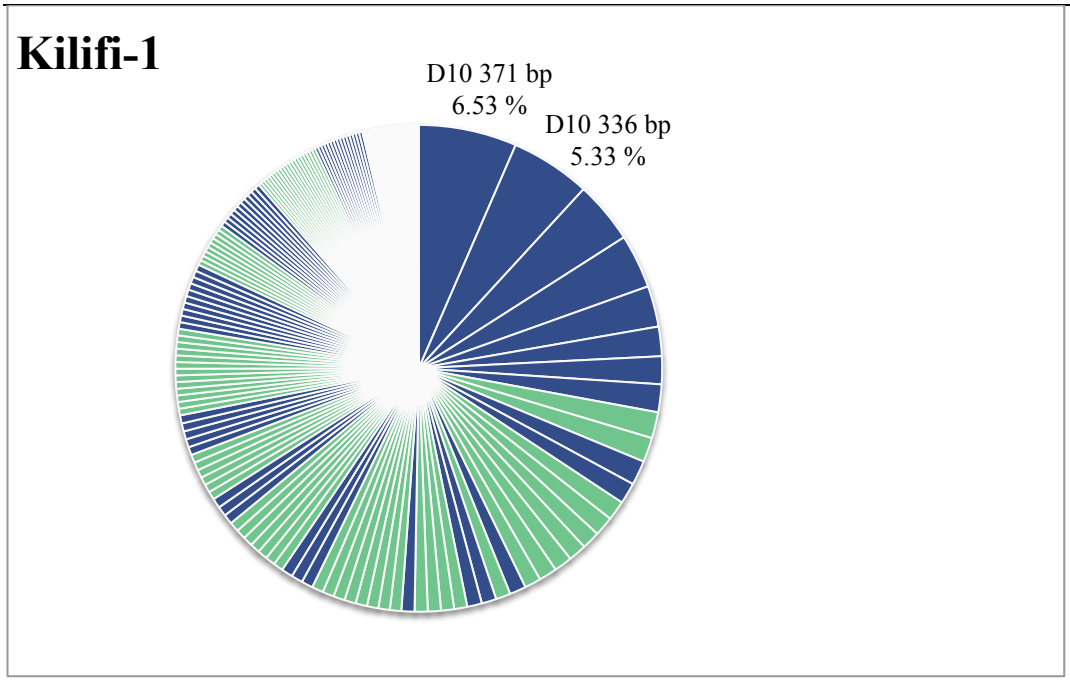

Figure 35: Allele frequencies Kilifi-1. Frequencies > 5 % are indicated with exact allele frequency, with fragment length and allelic type. The green colour depicts 3D7-type alleles and the blue colour represents D10-type alleles. Lengths of fragment are indicated as bp.

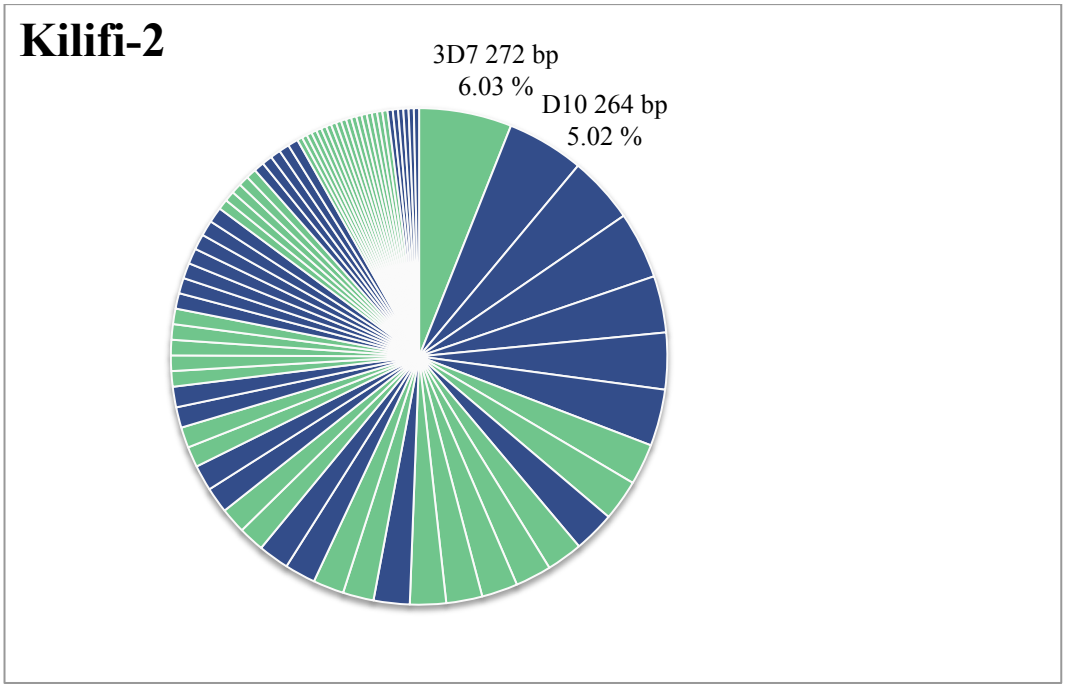

Figure 36: Allele frequencies Kilifi-2. Frequencies > 5 % are indicated with exact allele frequency, with fragment length and allelic type. The green colour depicts 3D7-type alleles and the blue colour represents D10-type alleles. Lengths of fragment are indicated as bp.

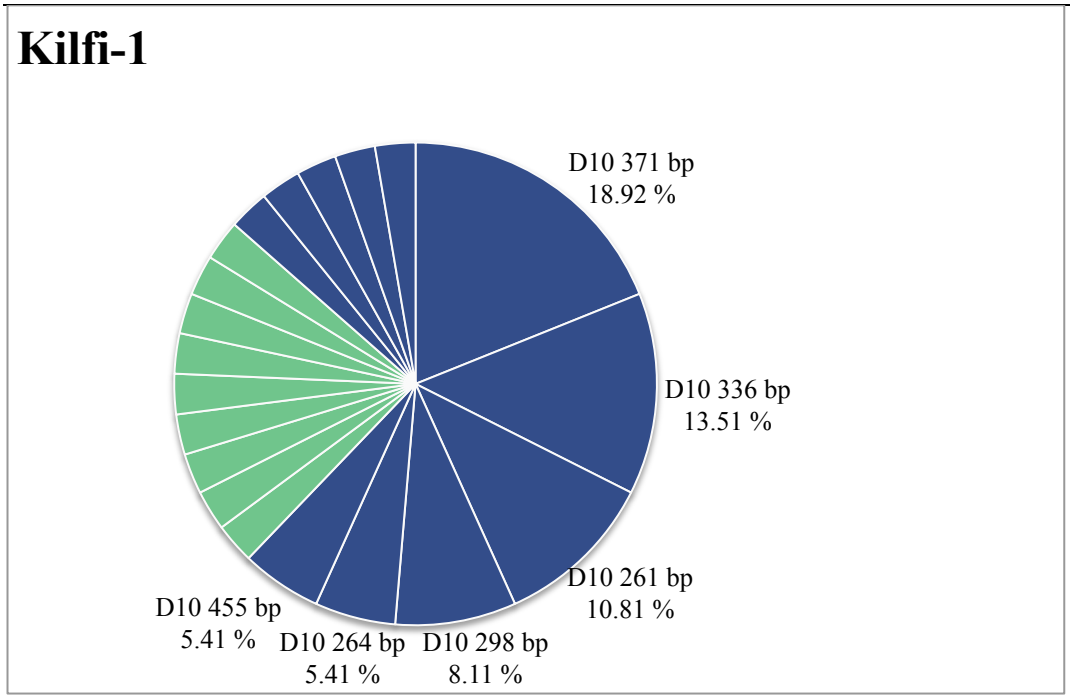

Figure 37: Allele frequencies of recrudescences in Kilifi-1. The genotypes are depicted in their respective frequencies and fragment length. The green colour depicts 3D7-type alleles and the blue colour represents D10-type alleles. Lengths of fragment are indicated as bp.

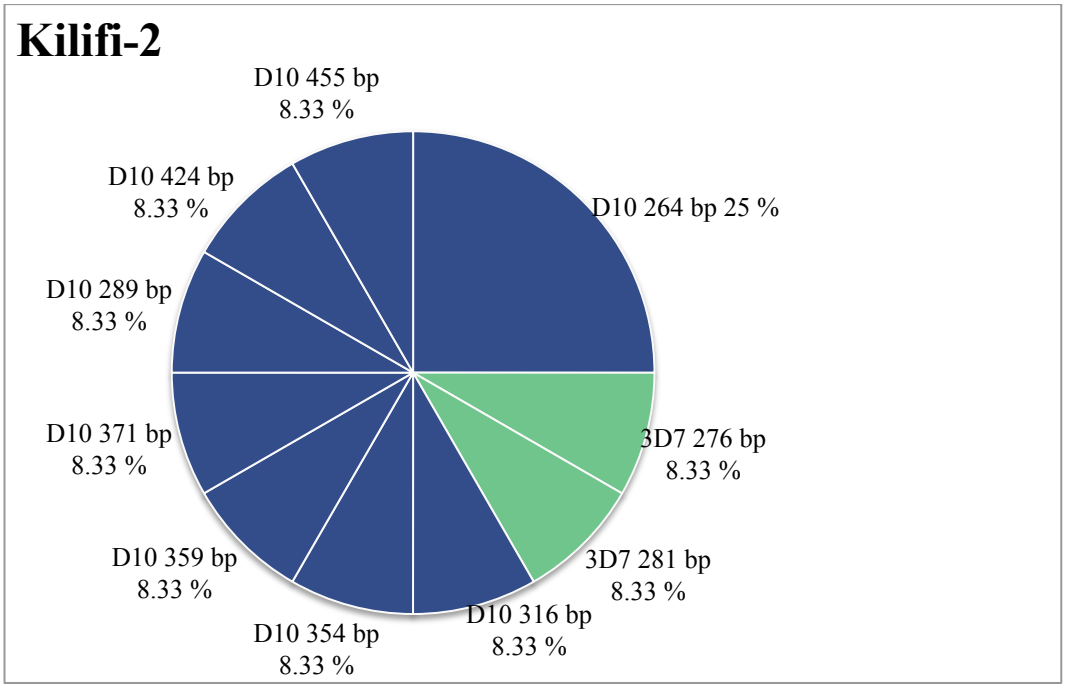

Figure 38: Allele frequencies of recrudescences in Kilifi-2. The genotypes are depicted in their respective frequencies and fragment length. The green colour depicts 3D7-type alleles and the blue colour represents D10-type alleles. Lengths of fragment are indicated as bp.

Acknowledgements

First of all, I want to thank the patients from Bobo-Dioulasso, who participated and made it possible to conduct the present study.

Thank you to Professor Abdoulaye Djimdé, the Project Coordinator in Bamako for making me become part of the WANECAM project. My special thanks to my Burkinabe supervisors: Professor Jean-Bosco Ouédraogo, who invited me to Bobo-Dioulasso and became a great host, to Issaka Zongo, the coordinator of the clinical part of the study in Bobo-Dioulasso and Fabrice Somé, the leader of the study's laboratory in Bobo-Dioulasso who was patient and helpful for both professional problems and personal information about the country. Also, I want to thank the whole team in Sakaby and Colsama: Dr. Compaoré who explained many medical and cultural things. The team of doctors, nurses, biologists, coordinators and drivers, who were great colleagues and in many cases became friends. I enjoyed working and laughing with you. Thank you for letting me become part of your team and for letting me share a wonderful time with you.

I am very grateful towards Professor Steffen Borrmann, who gave me the opportunity to spend a wonderful year in Burkina Faso while gaining experience in antimalarial research. Thank you for supervising and advising me. Also, I want to thank the laboratory team; Mamadou Tékété for your explanations, Martina Henk for the help at the laboratory in Tübingen; Nicole Peters in Magdeburg for the help in the preparation phase before going to Burkina Faso. Thank you to Nicole Peters and Anja Rippert in Heidelberg for providing the genotyping data from Kilifi, Kenya.

Besonders möchte ich auch meiner Familie und meinen Freunden danken, die mich in schwierigen Momenten unterstützt und bekräftigt haben. Vor allem danke ich meinen Eltern, die mich während meines gesamten Studiums unterstützt und die Dissertation Korrektur gelesen haben und Dennis, der mir beim Erstellen der Schemata geholfen hat und bei allen Höhen und Tiefen der schriftlichen Verfassung dieser Arbeit zur Seite stand.